

1995

Determination of appropriately sized principal component models and their effect on detection and isolation

David M. Himes
Lehigh University

Follow this and additional works at: <http://preserve.lehigh.edu/etd>

Recommended Citation

Himes, David M., "Determination of appropriately sized principal component models and their effect on detection and isolation" (1995). *Theses and Dissertations*. Paper 333.

This Thesis is brought to you for free and open access by Lehigh Preserve. It has been accepted for inclusion in Theses and Dissertations by an authorized administrator of Lehigh Preserve. For more information, please contact preserve@lehigh.edu.

AUTHOR:

Himes, David M.

TITLE:

**Determination of
Appropriately Sized
Principal Component
Models and Their Effect
on Detection and Isolation**

DATE: May 28, 1995

DETERMINATION OF
APPROPRIATELY
SIZED PRINCIPAL COMPONENT
MODELS
AND THEIR EFFECT ON
DETECTION AND ISOLATION

by
David M. Himes

A Thesis
Presented to the Graduate Committee
of Lehigh University
in Candidacy for the Degree of
Master of Science
in
Chemical Engineering

Lehigh University
1995

© Copyright 1995 by David M. Himes
All Rights Reserved

This thesis is accepted in partial fulfillment of the requirements for the degree of
Master of Science.

April 28, 1995
(Date)

Christos Georgakis
(Chemical Engineering)

Robert H. Storer
(Industrial and Manufacturing Systems Engineering)

Dennis W. Hess
(Chairman, Department of Chemical Engineering)

Acknowledgments

I would like to thank my thesis advisors Christos Georgakis and Robert Storer for their assistance and guidance with this work. I would also like to thank the Chemical Engineering Department, PMC, and the members of the IAC for providing the financial support and the opportunity for this project.

I owe a tremendous debt of gratitude to Wenfu Ku, my PCA mentor. His assistance with PCA, LaTeX, assorted computer problems, and X-Pilot strategies were invaluable in my completion of this work (and in keeping sane).

I also want to thank and at the same time curse, Phil Lyman, Tom Haynes, and Jake Fotopoulos for showing me the "Marches of Antan". Thanks are also due to Joel and Ellen Cantrell, Tim Elliot, and Tom Steinmetz for their support and friendship.

Above all I want to thank my wife Kathy and my son David. Thank you for your understanding and patience. This accomplishment is as much yours as it is mine. I love the both of you very much.

4

Contents

Acknowledgments	v
Abstract	1
1 Introduction	3
1.1 Principal Component Analysis	4
1.2 Scaling	5
1.3 Building a PCA Model	6
1.4 The Tennessee Eastman Process	7
2 Choosing Appropriately Sized PCA Models	9
2.1 Methods for Choosing Model Size	9
2.1.1 Variance Based Methods	9
2.1.2 Cross-Validation	11
2.1.3 Interpretation of Loading Vectors	14
2.2 Disturbance Detection	15
2.2.1 Controlling the False Alarm Rate	16
2.2.2 Sensitivity of Detection to Model Size	17
2.3 Disturbance Isolation	25
2.3.1 Empirical Approach	26
2.3.2 Numerical Approach	28
2.4 Summary	33

3	Decentralized PCA Models in Multivariate SPC	37
3.1	Decentralized PCA Method	37
3.2	Applications	38
3.2.1	Local Disturbance Compensation	38
3.2.2	Distributed Disturbance Compensation	43
3.2.3	Reduced Magnitude Disturbances	45
3.2.4	Control Structure Evaluation	47
3.3	Summary	49
	Bibliography	50
	A Nomenclature	55
	B Speed of Detection	57
	C Decentralized Charts	65
	Vita	78

List of Tables

1.1 Tennessee Eastman Step Disturbances	7
3.1 Division of Process Variables into Decentralized Units	39

List of Figures

1.1	Tennessee Eastman Process and Control Structure (Courtesy of Lyman)	8
2.1	Parallel Analysis for the Tennessee Eastman Process, Steady State Conditions. a) 100 Samples x 52 Variables, b) 1000 Samples x 52 Variables	10
2.2	Cross Validation for the Tennessee Eastman Process, Normal Operating Conditions	12
2.3	Eastment and Krzanowski Cross-Validation for the Tennessee Eastman Process, Steady State Conditions	13
2.4	Fraction of 5,000 Samples within 95% Empirical Control Limits	18
2.5	Speed of Detection for Tennessee Eastman Under Normal Operation versus Number of Components in the PCA Model	19
2.6	Speed of Detection for Tennessee Eastman Disturbance 1 versus Number of Components in the PCA Model	21
2.7	Speed of Detection for Tennessee Eastman Disturbance 4 versus Number of Components in the PCA Model	21
2.8	Monitoring Plots for the Tennessee Eastman Process Disturbance 4, Models based on All Measurements (top) and All Measurements Except the Reactor Cooling Water Return Valve (bottom).	22

2.9	Top plots: Speed of Detection for Tennessee Eastman Disturbance 1 at 20% Magnitude Reduction versus Number of Components in the PCA Model. Bottom plots: Q and T^2 Monitoring Plots for Reduced Magnitude Disturbance 1 (solid line) and Disturbance 1 (dashed line). (sampling interval = 3 minutes).	23
2.10	Top plots: Speed of Detection for Tennessee Eastman Disturbance 4 at 50% Magnitude Reduction versus Number of Components in the PCA Model. Bottom plots: Q and T^2 Monitoring Plots for Reduced Magnitude Disturbance 4 (solid line) and Disturbance 4 (dashed line). (sampling interval = 3 minutes).	24
2.11	Disturbance Detection and Isolation Plots for Tennessee Eastman Disturbances 1 (left), 4 (middle), and reduced magnitude 1 (right).	27
2.12	Parallel Analysis for the Tennessee Eastman Process, Disturbance Conditions. a) 100 Samples, b) 1000 Samples	29
2.13	Isolation Plots for Disturbance 1 Data Projected Against the New-Steady-State Disturbance 1 Model	30
2.14	Isolation Plots for a Disturbance 1 Data Projected onto a Disturbance 1 Model (top), a Disturbance 4 Model (middle), and a Reduced Magnitude Disturbance 1 Model (bottom).	31
2.15	Isolation Plots for a Disturbance 4 Data Projected onto a Disturbance 1 Model (top), a Disturbance 4 Model (middle), and a Reduced Magnitude Disturbance 1 Model (bottom).	32
2.16	Isolation Plots for Reduced Magnitude Disturbance 1 Data Projected onto a Disturbance 1 Model (top), a Disturbance 4 Model (middle), and a Reduced Magnitude Disturbance 1 Model (bottom).	32
2.17	Parallel Analysis and Cross-Validation for Data Scaled by Measurement Span	34
3.1	Centralized Monitoring of TE Disturbance 4, Reactor Cooling Water Inlet Temperature Step Change	40

3.2	Decentralized Monitoring of TE Disturbance #4, Reactor Cooling Water Inlet Temperature Step Change	41
3.3	Decentralized Monitoring of TE Disturbance #5, Condenser Cooling Water Inlet Temperature Step Change	42
3.4	Decentralized Monitoring of TE Disturbance #6, A Feed Loss (Stream 1)	44
3.5	Decentralized Monitoring of TE Disturbance #1, Composition Step Change (Stream 4)	46
3.6	Decentralized Monitoring of TE Reduced Magnitude Disturbance #1, Composition Step Change (Stream 4)	48
B.1	Speed of Detection versus Number of Components in the PCA Model. Disturbance 1 (top plots), Reduced Magnitude Disturbance 1 (middle plots), Monitoring Plots (bottom).	59
B.2	Speed of Detection versus Number of Components in the PCA Model. Disturbance 2 (top plots), Reduced Magnitude Disturbance 2 (middle plots), Monitoring Plots (bottom).	60
B.3	Speed of Detection versus Number of Components in the PCA Model. Disturbance 4 (top plots), Reduced Magnitude Disturbance 4 (middle plots), Monitoring Plots (bottom).	61
B.4	Speed of Detection versus Number of Components in the PCA Model. Disturbance 5 (top plots), Reduced Magnitude Disturbance 5 (middle plots), Monitoring Plots (bottom).	62
B.5	Speed of Detection versus Number of Components in the PCA Model. Disturbance 6 (top plots), Reduced Magnitude Disturbance 6 (middle plots), Monitoring Plots (bottom).	63
B.6	Speed of Detection versus Number of Components in the PCA Model. Disturbance 7 (top plots), Reduced Magnitude Disturbance 7 (middle plots), Monitoring Plots (bottom).	64
C.1	Decentralized Monitoring of TE Disturbance #1	66
C.2	Decentralized Monitoring of TE Reduced Magnitude Disturbance #1	67

C.3	Decentralized Monitoring of TE Disturbance #2	68
C.4	Decentralized Monitoring of TE Reduced Magnitude Disturbance #2	69
C.5	Decentralized Monitoring of TE Disturbance #4	70
C.6	Decentralized Monitoring of TE Reduced Magnitude Disturbance #4	71
C.7	Decentralized Monitoring of TE Disturbance #5	72
C.8	Decentralized Monitoring of TE Reduced Magnitude Disturbance #5	73
C.9	Decentralized Monitoring of TE Disturbance #6	74
C.10	Decentralized Monitoring of TE Reduced Magnitude Disturbance #6	75
C.11	Decentralized Monitoring of TE Disturbance #7	76
C.12	Decentralized Monitoring of TE Reduced Magnitude Disturbance #7	77

Abstract

This thesis presents the results of research into the effect size has on the ability of a principal component model to detect and isolate a disturbance. In the first part of this paper, I explored how model size as determined by the number of components retained effects detection and isolation procedures. In the second part, I explored the decentralized approach to process monitoring. That is, investigating whether models developed from a smaller but perhaps more closely related set of variables can be an additional tool in statistical process control (SPC).

The Tennessee Eastman simulation was used as a test case. This simulation was developed by Downs and Vogel in 1993 as a challenge problem in the area of plant-wide industrial process control. A series of possible disturbances were included with this program. However, it was found that they were, for the most part, quite large and posed no significant challenge to SPC. Many of the examples presented in this paper represent cases in which the disturbance magnitudes were reduced in order to fully test the proposed SPC methods.

Chapter 1

Introduction

Principal component analysis (PCA) is a technique used in many disciplines for the purposes of multivariable statistical analysis. The application of PCA as a tool for statistical quality control was first presented in a paper by Jackson in 1959 [9]. The usefulness of this technique in the realm of SPC lies in its ability to separate systematic variation from noise and collinearity in process measurements. This separation leads to a reduction of dimensionality. Instead of monitoring each process measurement individually, process monitoring can be performed on two charts, one for the systematic variation, T^2 and one for the noise, Q .

In an industrial application, all measurements corresponding to a single process and/or product line are utilized in developing a centralized PCA model. Despite the substantial order reduction afforded by centralized PCA models, additional benefits might be derived by the development of decentralized PCA models. This is motivated by the fact that processes often consist of well identified process units. These units are sequentially arranged but are also highly interconnected through the existence of one or several recycle streams. Depending on the effectiveness of the control structure, disturbances can propagate throughout the plant or be quickly compensated and their effect on the rest of the plant eliminated close to their source.

In the decentralized PCA approach, which the second part of this thesis describes, a model was developed for each unit in the process. It was theorized that the control chart of the unit in which the disturbance originated would go out of

control first, indicating that decentralized PCA charts could be used to not only detect a disturbance but also to isolate it. It was found that how a disturbance propagated and what effect it had on the remaining decentralized PCA charts depended on the dynamics of the process, the nature of the disturbance and the quality of the control structure. The use of these decentralized charts to isolate the root cause of the disturbances was also examined.

Regardless of whether the monitoring is centralized or decentralized, a key step in performing the analysis was deciding how many of the components to include in the principal component model, i.e. what was the dividing line between the systematic variation and the noise. Jackson [10] provided a review of the many methods that have been conceived for the purpose of choosing components. Recent research, however, had indicated that models developed with no more than two or three components were successful for disturbance detection and isolation [12, 13, 17]. In the first part of this thesis, the sensitivity of detection speed and accuracy of isolation to the size of principal component model was analyzed.

The Tennessee Eastman (TE) Process simulation [2] was used as a case study for this investigation.

1.1 Principal Component Analysis

The method for calculating the principal components is usually expressed as a decomposition of the vector space X , a matrix of m samples on n variables, into smaller vector spaces called loadings, P , and scores, T . The loadings vectors represent the principal component orientations in the n variable dimensional space. These vectors are orthogonal to each other and are, therefore, also referred to as principal axes. The scores vectors represent the distribution of the m samples projected along each loading vector. These vectors are called the principal components. Using the notation of Wise et al. [20] and Kresta et al. [13]:

$$X = TP^T = t_1p_1^T + t_2p_2^T + t_3p_3^T + \dots + t_np_n^T \quad (1.1)$$

1.2. SCALING

This decomposition is equivalent to performing a Singular Value Decomposition, SVD.

$$X = U\Sigma V^T \quad (1.2)$$

where $T = U\Sigma$ and $P = V$. The matrix Σ is diagonal with the entries equal to the standard deviation for each principal component. The matrix U is called the left singular vector matrix. Because the SVD can be difficult for large matrices, the procedure is usually performed on the covariance matrix S of the vector space X .

$$S = \frac{X^T X}{m - 1} \quad (1.3)$$

$$S = V\Lambda V^T \quad (1.4)$$

In this case, the entries of the diagonal matrix Λ are equal to the variance of the respective principal components. The scores are calculated by:

$$T = XV \quad (1.5)$$

The first principal component is defined by the scores vector whose loadings vector is oriented in the direction of maximum variance. The second principal component has a loadings vector which is oriented in the direction of maximum remaining variance. The third principal component is determined in the same manner, and so on until the total variance of X has been explained by the principal components.

1.2 Scaling

Scaling of the data has a significant impact on the results of PCA. In SPC for chemical processes the data are typically of different types, i.e. temperatures, compositions, valve positions. In addition, the units of measure for each variable are not unique. For example, it is possible to perform a linear transformation to change a temperature variable from units of Fahrenheit to units of Celsius. Associated with such transformations is a change in the variance of that variable. This in turn changes the total variance for the vector space, stretching the space in artificial directions.

Hotelling addressed this issue in a 1933 article [8] presenting a method of computing principal components. He asserted that the method of principal components is based on the assumption that the variance of each measurement is unity. This scaling bounds the total variance of the vector space equal to the number of variables in that space. When the data are centered and scaled in this fashion it is called auto-scaling.

Hotelling concedes, however, that other types of scaling may also be appropriate. Alternative scaling [13, 12] would include production specifications for product variables, controller ranges for control inputs, and instrument ranges for other variables. Variables of the same type, e.g. compositions from an analyzer, should all be scaled equally so that their natural relationships are not affected. Additionally, Kresta et al. [13] cautions against scaling up the variance of near constant variables.

1.3 Building a PCA Model

The principal component matrix, Y is calculated by:

$$Y = XW_k \quad (1.6)$$

where W_k is given by:

$$W_k = V_k \Lambda_k^{-1/2} \quad (1.7)$$

The subscript k denotes the size of the PCA model W . The eigenvectors V are scaled by their eigenvalues Λ so that the principal components will have unit standard deviation. This scaling was suggested by Jackson and Mudholkar [11] as convenient for future calculation of control limit statistics (see Section 2.2).

It is desired that the size of the PCA model is such that the “retained” principal components are representative of the total process variation. The eigenvectors not included in the PCA model represent a set of linear constraints on the process variation. In the absence of noise, auto-correlation and nonlinearity these collinear relations would be given exactly by the eigenvectors related to principal components with zero variance. In industrial applications, this will probably not be the case and

1.4. THE TENNESSEE EASTMAN PROCESS

Table 1.1: Tennessee Eastman Step Disturbances

#	Description
1	A/C Feed Ratio, B Composition Constant (stream 4)
2	B Composition, A/C Ratio Constant (stream 4)
3	D Feed Temperature (stream 2)
4	Reactor Cooling Water Inlet Temperature
5	Condenser Cooling Water Inlet Temperature
6	A Feed Loss (stream 1)
7	Header Pressure Loss - Reduced Availability

the choice of model size will be more difficult. Some methods available for choosing model size are reviewed in Chapter 2.

1.4 The Tennessee Eastman Process

This examination of principal component analysis made use of data generated by a plant simulation developed by Downs and Vogel of the Tennessee Eastman Company [2]. This Tennessee Eastman (TE) process includes five operation units: a two phase reaction vessel, a condenser, a separator, a recycle compressor, and a stripper. Four exothermic gas phase reactions are modeled, producing two products and two by-products. The output from the simulator consists of 41 process measurements and 12 manipulated variables from controllers.

This simulation was developed as an industrial challenge problem for plant-wide control. Lyman et al. [19, 18, 16] developed several control structures for this process. This paper makes use of Lyman's control structure #2, which was found to be the most effective with respect to disturbances included in the TE simulation (see Table 1.1). This structure fixes the reactor agitator speed to a constant value. As a consequence of this, the number of variables available for use in SPC is 52. Figure 1.1 illustrates the process and its control structure.

It turned out that the data generated by this simulation was severely auto-correlated. This auto-correlation had a negative affect on the static PCA model

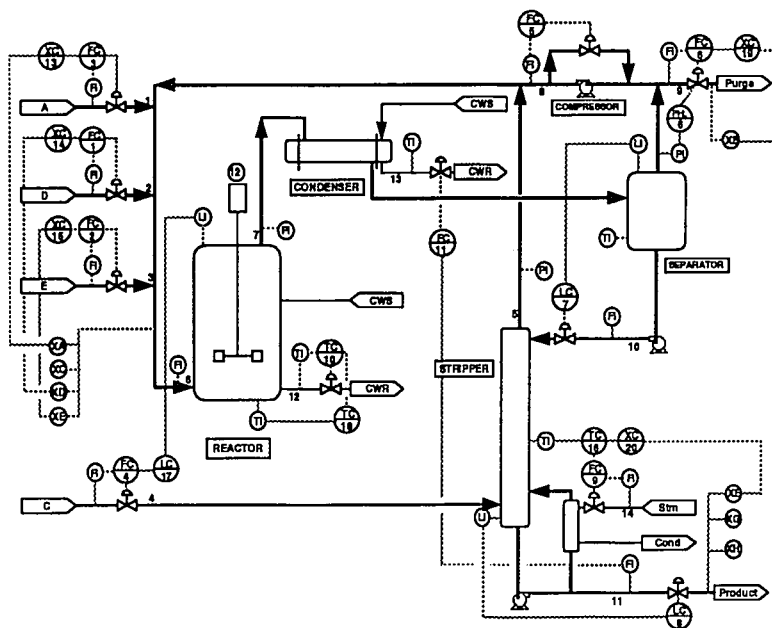


Figure 1.1: Tennessee Eastman Process and Control Structure (Courtesy of Lyman)

development described in Section 1.3. In order to minimize this detrimental effect a sampling interval of three minutes was chosen for all examples in this paper. However, treatment of auto-correlated systems is possible through development of a dynamic PCA model [15].

Chapter 2

Choosing Appropriately Sized PCA Models

2.1 Methods for Choosing Model Size

2.1.1 Variance Based Methods

There are many available methods for choosing components, most involving a number of assumptions about the variance of each component. Under auto-scaling, the total system variance is constrained to the number of system variables; 52 in the case examined in this paper. Thus the sum of the variances of the principal components must also equal 52. The portion of total variance explained by each principal component is given by the corresponding eigenvalue of the covariance matrix for the process data.

The amount of variance attributed to noise may be known in some systems, thereby allowing the choice of components based on the percentage of variance to be covered by the PCA model. In the TE application this was not the case. However, 99% of the total TE system variance was coverable by 40 components, indicating that 12 components represent a noiseless collinearity.

In 1966 Cattell published observations he made about covariance eigenvalue distributions [1]. Plots of the covariance eigenvalues versus their respective component

CHAPTER 2. CHOOSING APPROPRIATELY SIZED PCA MODELS

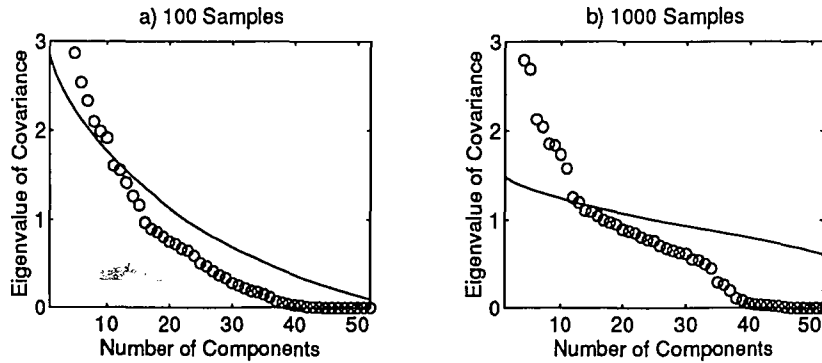


Figure 2.1: Parallel Analysis for the Tennessee Eastman Process, Steady State Conditions. a) 100 Samples x 52 Variables, b) 1000 Samples x 52 Variables

number tended to have a characteristic shape. Cattell found that the first few components had large eigenvalues and their values dropped off rapidly to a bend in the curve. The eigenvalues that followed dropped off much slower, sometimes falling in a single straight line or a series of lines joined by short drops. He named these latter components “scree”, a geological term referring to the rocky rubble at the bottom of a cliff.

In 1965, Horn published a method in which the process covariance eigenvalues were compared with their expected values if the measurements were completely uncorrelated [7]. A plot of the eigenvalues of both sets of data as a function of the number of principal components yielded two curves that intersect. It was the intersection which separated the components for use in the model from those representing system constraints. In the case of infinite sampling, the uncorrelated set of auto-scaled variables would have generated a covariance matrix having all unit eigenvalues. This criterion was named “latent-root-one” or K-1 test.

Examples of the parallel analysis procedure are presented in Figure 2.1. A comparison is made between the use of 100 samples versus 1000 samples. The TE data is represented by open circles and the uncorrelated data is represented by solid lines. Note that the eigenvalues for the first few components do not fall within the scale of the figures. In the 100 sample case, parallel analysis indicates that 10 components should have been retained. In the 1000 sample case, parallel analysis indicates that

2.1. METHODS FOR CHOOSING MODEL SIZE

13 components should have been retained. This comparison illustrates that when additional samples were used, resolution between constraining relations which were noisy (components 13-39) and those which were essentially noise free (components 40-52) improved.

2.1.2 Cross-Validation

Cross-validation is a method in which PCA models of varying size are analyzed for their ability to predict the original data [21, 3]. It is generally assumed that process data will contain some cross-correlation, resulting in the final principal components representing the system collinearity, albeit corrupted by noise. The prediction of the original data is expected to improve with increasing model size up to the collinear components; at which point no unique information remains. It has been shown for Partial Least Squares [4] that a minimum error in prediction will occur at the collinearity. The addition of collinear components adds only noise, thereby increasing prediction error.

The cross-validation procedure used in this paper is referred to as PRESS, *P*redicted *E*rror *S*um of *S*quares. It is, mathematically: the average of the sum of the squared error or residual between a set aside portion of data and predicted data, based on a model built without the set aside data.

$$PRESS(k) = \frac{1}{mn} \sum_{i=1}^m \sum_{j=1}^n (\hat{x}_{ij}^{(k)} - x_{ij})^2 \quad (2.1)$$

The predicted data, \hat{x}_{ij}^k , is calculated through the relation:

$$\hat{x}_{ij}^k = x_{ij} V_k V_k^T \quad (2.2)$$

Once this is done for each size model, a new subset of samples is chosen to set aside and the PCA models are based on the remaining samples. This calculation is performed repeatedly until all samples have been included in the subset once. The results for each iteration are then averaged and the component at which the PRESS is minimized identifies the appropriate model size.

CHAPTER 2. CHOOSING APPROPRIATELY SIZED PCA MODELS

There are various ways in which to choose the subset of samples. Groups can be chosen in sequential blocks or randomly with or without replacement. No significant differences in the results were found for the TE process from the different grouping schemes.

This cross-validation method is demonstrated in Figure 2.2 for the TE Process under steady state conditions. It was found that this procedure was not overly sensitive to sample sizes of 100 and up for TE data. This was shown not to be true, in general, for the variance based methods (see Figure 2.1). Nor was it true for disturbance data where the amount of transient data included in the model effected the results (see Section 2.3.2).

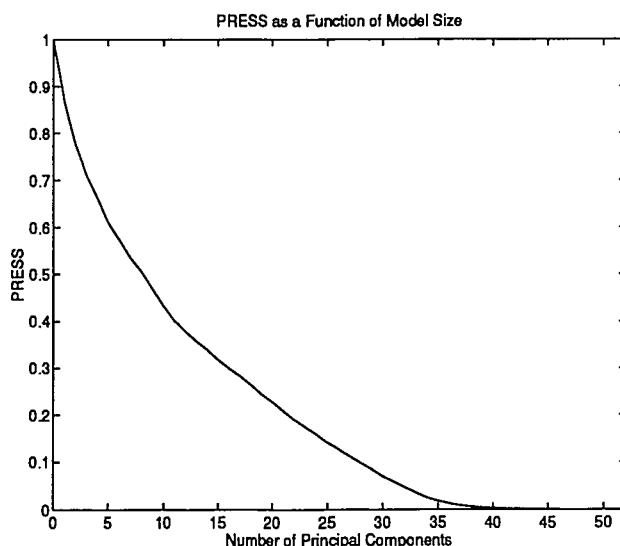


Figure 2.2: Cross Validation for the Tennessee Eastman Process, Normal Operating Conditions

Figure 2.2 also shows that the minimum PRESS occurred at the final component. In cases like these, the location at which the PRESS essentially reaches a zero value is generally taken as the number of components to retain. For the TE system, then, cross-validation indicated that 40 components should be retained. The remaining 12 components represented the system collinearity. This result was perhaps not surprising since the last components had near zero variance, see Figure 2.1.

2.1. METHODS FOR CHOOSING MODEL SIZE

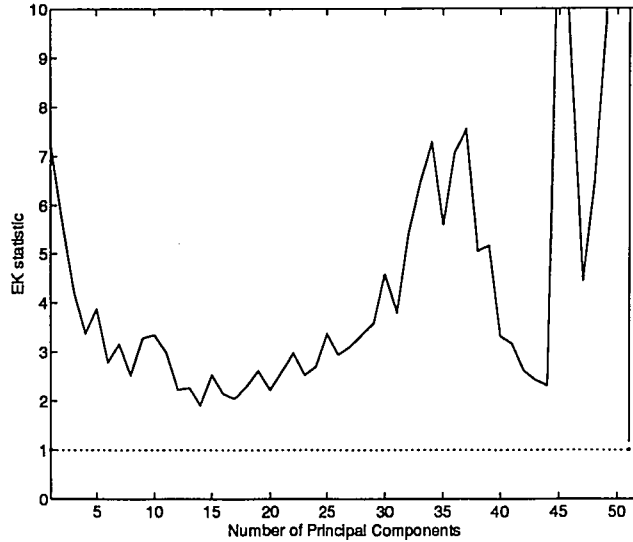


Figure 2.3: Eastment and Krzanowski Cross-Validation for the Tennessee Eastman Process, Steady State Conditions

Other authors believe that the PRESS statistic alone is not adequate for choosing the size of the PCA model but that some method of comparing successive PRESS values is needed. One such method has been suggested by Eastment and Krzanowski [3]:

$$EK_k = \frac{(PRESS(k-1) - PRESS(k))/D_k}{PRESS(k)/D_r} \quad (2.3)$$

where

$$D_k = m + n - 2k \quad (2.4)$$

is the degrees of freedom needed to fit the k^{th} component and

$$D_r = n(m-1) - \sum_{i=1}^k (m+n-2i) \quad (2.5)$$

is the remaining degrees of freedom after the fit. For the k^{th} component to contribute significant information to the model, W_k the statistic EK_k should have a value greater than unity.

The results of this procedure are illustrated in Figure 2.3. It can be seen from this figure that this method suggested that all the components should be retained

CHAPTER 2. CHOOSING APPROPRIATELY SIZED PCA MODELS

in the model. This result was rejected, though, since the last 12 components clearly would have contributed nothing to the model.

2.1.3 Interpretation of Loading Vectors

A more insightful method of choosing components is to attempt to identify or interpret the loading vectors corresponding to system constraints. It is useful to consider three component types identified by the parallel analysis method. In the first parallel analysis region, principal components have variances in excess of what would be expected of a set of uncorrelated variables. The second region includes principal components which have variances characteristic of uncorrelated variation. The loading vectors associated with these components will have random orientations, making them uninterpretable physically. The last region of components is associated with the system constraint. The variance of these components is dependent upon the degree to which noise corrupts the linear relationships between the original variables.

There were two sources of constraining relationships for the TE process. The first type of constraint was the chemical/physical relationship which links the process variables, i.e. mass balances, stoichiometry of reactions, thermodynamic relationships. The second source was the control structure for the process. An examination of the process data revealed that most of the loading vectors corresponding to the third parallel analysis region had large loadings for the manipulated variables. This seemed to indicate that the control structure played a significant role in constraining the process. In fact, it was possible to accurately identify several controller relationships from the loading vectors. It is interesting to note that some of the manipulated variables, which are valve positions, did not have significant loadings, possibly indicating that these valves were nonlinear.

There were several sources of noise affecting the constraining relations for the TE process. The first type was measurement noise which was added to each of the 41 process measurements but not the 11 manipulated variables. Thus, the measurement noise only affected the chemical/physical constraint. Some of the noise affecting the

2.2. DISTURBANCE DETECTION

controller relationships was due to the dynamic nature of the integral portion of the controllers. Note that these dynamic relations can be obtained by using a dynamic PCA technique [15]. An additional source of noise was related to the continuous change of controller set-points by the master-control portion of the seven cascade control loops. This caused the constraining relations themselves to be noisy.

The principal components 40-52 had near zero variances. The loading vectors corresponding to these components were easily identifiable as constraining relationships and were believed to be mainly controller relationships. These obviously did not belong in the PCA model. The questionable components were 16-39. These components had variances ranging from near random to near zero. Parallel Analysis rejected them, PRESS included them, and noise concealed their interpretation. In addition, each constraining relation could have included multiple physical relationships, making identification even more difficult.

2.2 Disturbance Detection

The on-line monitoring of the process can begin once the model size is chosen. As new data are collected from the process, they are scaled with the mean and standard deviation of the model data. The single sample is then projected onto the principal component model to generate the new principal component values.

$$y_{new,k} = x_{new} W_k \quad (2.6)$$

The occurrence of a disturbance is indicated by the violation of the two model based control limits, T^2 and Q . The control statistic T^2 , when the eigenvectors are scaled according to Equation 1.6, is simply the sum of squares of the principal components for a particular time instance.

$$T^2 = y_{new,k}^T y_{new,k} \quad (2.7)$$

A violation of the control limit for this statistic would be an indication that the new data has variance in excess of the model data. The control statistic Q , the sum of

CHAPTER 2. CHOOSING APPROPRIATELY SIZED PCA MODELS

the squares of the residual is given by:

$$Q = \epsilon^T \epsilon \quad (2.8)$$

where the residual, ϵ is given by:

$$\epsilon = x_{new}(I - V_k V_k^T) \quad (2.9)$$

A violation of the Q control limit would indicate that the new data no longer "fits" the model, W_k .

Unfortunately, there is still some uncertainty about how many components to retain for the model. Different methods can indicate different sized models; but it is not known if this matters. In other words, if the PCA model's ability to detect and isolate a disturbance is not very sensitive to the number of retained components, then any available method for choosing components would be adequate. The following sections present the development and execution of a sensitivity study which investigated this issue for the TE process.

2.2.1 Controlling the False Alarm Rate

As a first step in analyzing the sensitivity of detection to model size, it was necessary to verify that the control limits were producing approximately the same number of false alarms for each size model. This verification was necessary because of the effect that false alarms would have had on the sensitivity analysis. The analysis was based on the average of the first out of control sample detected after disturbance initiation (see Section 2.2.2). Some of these detections, however, might have been false alarms. False alarm detection would have occurred before the disturbance actually forced the process out of statistical control. The averaging of multiple simulations of the same disturbance, but using different random seeds, was used to mitigate some of the effects of detecting false alarms. However, if two models which should have actually detected the disturbance at the same time had different false alarm rates, then the one with the greater false alarm rate would have appeared to detect faster. This would have biased the sensitivity study to models with higher false alarm rates.

2.2. DISTURBANCE DETECTION

Proper control limits were needed for each model size in order to obtain equivalent false alarm rates. Following the advice of Ku et al. [15] and Wise et al. [20] for auto-correlated and or non-linear processes, the T^2 and Q control limits were set empirically. In this way, the assumptions regarding the distributions used in the development of the standard control limit calculations proposed by Jackson et al. [9, 11] were avoided.

The models, on which the control limits were based, were comprised of 5,000 samples of steady state operation, collected every three minutes. A model was generated for each of the possible number of principal components retained, i.e. 1, 2, ... $n - 1$ component models. Only $n - 1$ models were investigated because if the PCA model contained all n components, there would be no residual.

Next, 5,000 new samples were collected by running the simulation with a different random seed. Based on 95% type I error risk, the number of T^2 and Q false alarms were counted. Ideally, the fraction of samples in control should have been distributed about 0.95 for all model sizes. For the purposes of this study, however, it was only necessary that the fraction was approximately constant across model size, i.e. a controlled false alarm rate. The actual results of this analysis are presented in Figure 2.4. It can be seen from the Q chart that although the 95% confidence was not attained, the false alarm rate was relatively constant across model size. In the case of the T^2 statistic there was a slight trend towards increased false alarms with model size. This trend indicated a possible bias in the sensitivity results in Section 2.2.2 based on the T^2 statistic. The non-attainment of 95% confidence was attributed to the auto-correlation which was still present in the data despite the three minute sampling interval.

2.2.2 Sensitivity of Detection to Model Size

The next step in the procedure was to determine the ability of each size PCA model to detect a disturbance. These models were based on the 5,000 samples which were used to calculate the control limits in validation of the false alarm rate. Again, empirical control limits with 95% type I error risk were calculated with the

CHAPTER 2. CHOOSING APPROPRIATELY SIZED PCA MODELS

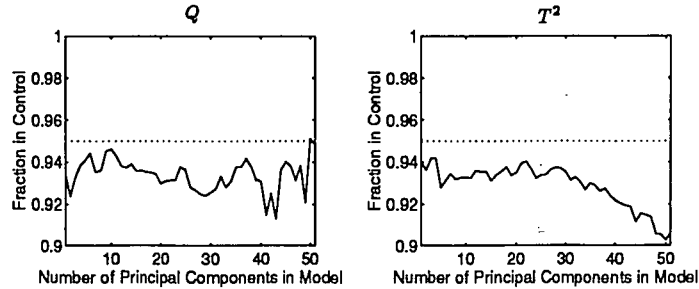


Figure 2.4: Fraction of 5,000 Samples within 95% Empirical Control Limits

assumption that the false alarm rate trend would not be significant.

For the TE disturbances, an attempt was made to determine if a certain size model would consistently detect the disturbance first. The procedure outlined below is an improvement upon one that presented in a previous paper [6]. In this case, the simulation was run 100 times for each of the disturbances instead of just once. For each of these runs, 80 samples were collected at three minute intervals after the initiation of the disturbance. The samples were projected onto the model and the error space and the T^2 and Q values were calculated for control limit violation evaluation. The first violation was designated as the sample at which the disturbance was first detected. These data were then averaged for the mean sample number of detection. In addition, an overall detection "chart" was used since a violation in either T^2 or Q is sufficient for detection. This was done for each run and every model size. This improvement allowed an averaging out of the effects of false alarms.

Ku et al. [15] demonstrated that the TE randomly varying disturbances tended to go out of statistical control later than the TE step disturbances, allowing more time for false alarms. It was also felt that the random variation type would have greater variance in time to go out of control. Realizing that this would have an adverse affect on the mean sample of detection, the decision was made to conduct the procedure for just the step disturbances. Additionally, TE disturbance numbers 3 and 9 were not investigated since Ku et al. found them to be undetectable.

2.2. DISTURBANCE DETECTION

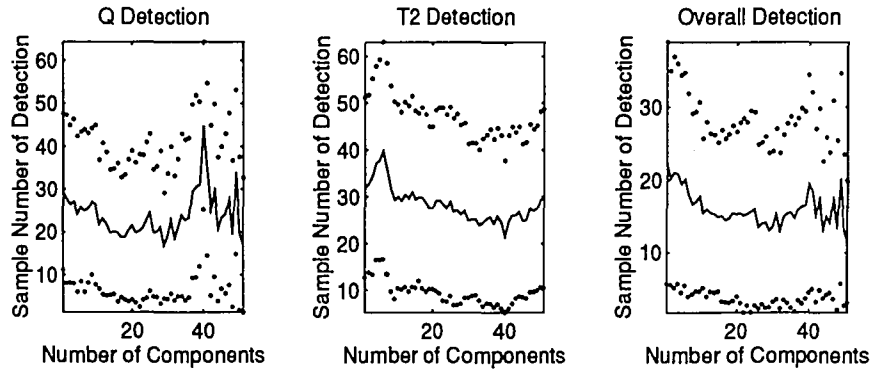


Figure 2.5: Speed of Detection for Tennessee Eastman Under Normal Operation versus Number of Components in the PCA Model

Occasionally a detection did not occur within the 80 samples which were collected. When this occurred, a temporary sample-of-detection number, η , was assigned. At the end of all the runs, these numbers were reassigned according to the following procedure:

$$\bar{\eta} = \bar{\eta}_N + f(80 - \bar{\eta}_N) \quad (2.10)$$

where $\bar{\eta}$ = the reassigned value, $\bar{\eta}_N$ = the average of the uncensored sample-of-detection numbers, f = the fraction of the data which is censored, and 80 is the average run length.

Figure 2.5 shows the results of this analysis for the TE process under normal operating conditions. The left plot represents the ability of the Q statistic to detect. The middle plot is for T^2 , and the right plot is for the overall. The solid line indicates the average sample at which a detection occurred. The dotted line indicates the standard deviation. This case was done principally as a reference for the disturbance cases. However, the results indicate that there was no trend in the detection of the first false alarm. Therefore it can be assumed that the occurrence of false alarms did not significantly impair the sensitivity study as was feared based on the T^2 results presented in Figure 2.4.

Figure 2.6 shows the results of this analysis for disturbance 1, a compositional

CHAPTER 2. CHOOSING APPROPRIATELY SIZED PCA MODELS

step change in the feed to the stripper. It can be seen from the overall plot that detection of this disturbance was possible regardless of model size. Additionally, there is a clear indication that a model with 34 components detected on average almost two samples faster than a one component model. This represents an insignificant detection delay of six minutes, which may have more to do with how the disturbance affected certain components than any indication of "true" model size.

It was found that the results for TE disturbance 1 were representative of the other step disturbances. In each case overall detection was possible for all models and there was little or no sensitivity in detection speed.

Figure 2.7 shows the results of this analysis for TE disturbance 4, a step change to the reactor cooling water inlet temperature. This disturbance generated unique Q and T^2 statistic results in comparison with the other analyzed step disturbances. The plots show that detection was difficult or impossible with T^2 until the model contained 30 components and detection was difficult or impossible with Q for models with 30 or more components. The fact that not all components were affected by the disturbance suggests that the local control structure was compensating for the majority of the disturbance.

To test this hypothesis two models were developed. The first model was based on all 52 measurements. The second model omitted the measurement for the reactor cooling water return valve, the variable most likely to have been affected by disturbance 4. Both models were comprised of 14 principal components. Thus, because T^2 only detected this disturbance with a 30+ component model, the disturbance was expected to have been detectable only on the Q chart for a 14 component model. Then the disturbance data was projected onto both models, the disturbance entering at sample 20. The results are presented in Figure 2.8. In the full measurement case Q clearly detected the disturbance and T^2 did not. In the case where the cooling water valve measurement was neglected, Q did not detect the disturbance. This result confirms that the local control action compensated for the disturbance.

The obvious onset of the disturbance, as indicated in the 52 measurement Q chart of Figure 2.8, highlights an important point about the simulation. The Tennessee Eastman process was developed to be a challenge for plant-wide control strategies.

2.2. DISTURBANCE DETECTION

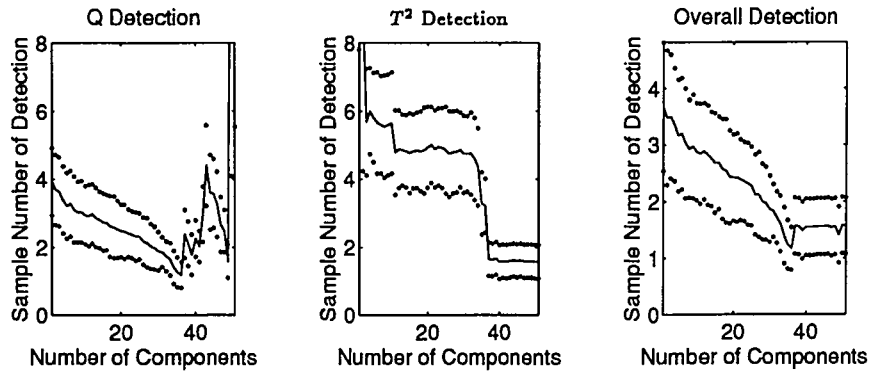


Figure 2.6: Speed of Detection for Tennessee Eastman Disturbance 1 versus Number of Components in the PCA Model

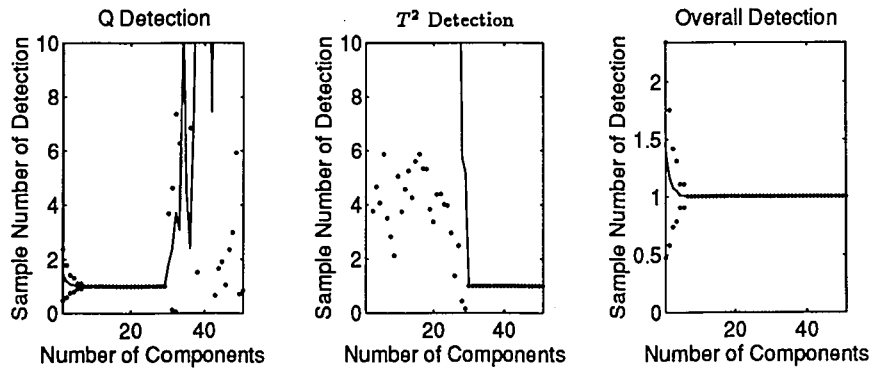


Figure 2.7: Speed of Detection for Tennessee Eastman Disturbance 4 versus Number of Components in the PCA Model

CHAPTER 2. CHOOSING APPROPRIATELY SIZED PCA MODELS

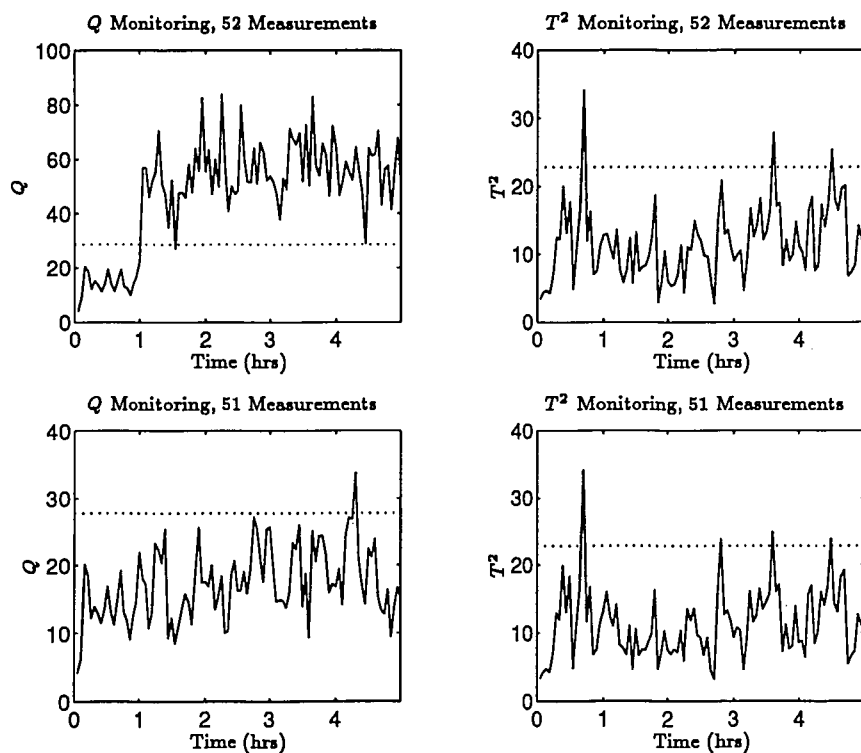


Figure 2.8: Monitoring Plots for the Tennessee Eastman Process Disturbance 4, Models based on All Measurements (top) and All Measurements Except the Reactor Cooling Water Return Valve (bottom).

2.2. DISTURBANCE DETECTION

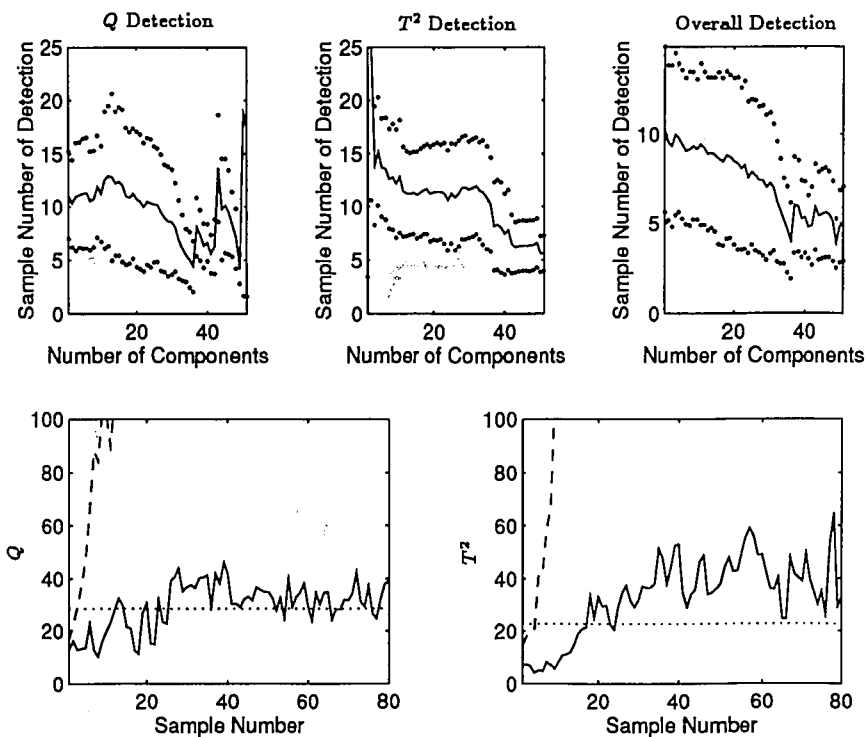


Figure 2.9: Top plots: Speed of Detection for Tennessee Eastman Disturbance 1 at 20% Magnitude Reduction versus Number of Components in the PCA Model. Bottom plots: Q and T^2 Monitoring Plots for Reduced Magnitude Disturbance 1 (solid line) and Disturbance 1 (dashed line). (sampling interval = 3 minutes).

It was assumed that part of this challenge involves disturbances that are large and difficult for controllers to immediately compensate. This means that the Tennessee Eastman disturbances are not likely to be very challenging for statistical process control tasks because of their substantial magnitudes. In an attempt to remedy this, the magnitude of some of the Tennessee Eastman disturbances was reduced and the analysis repeated.

Figure 2.9 shows the results of this analysis for disturbance 1 at 20% of its original magnitude. The speed of detection trends observed for the full magnitude case (see Figure 2.6) repeated here, only with a larger time scale. There is still a clear indication that a model with about 34 components detected on average faster than

CHAPTER 2. CHOOSING APPROPRIATELY SIZED PCA MODELS

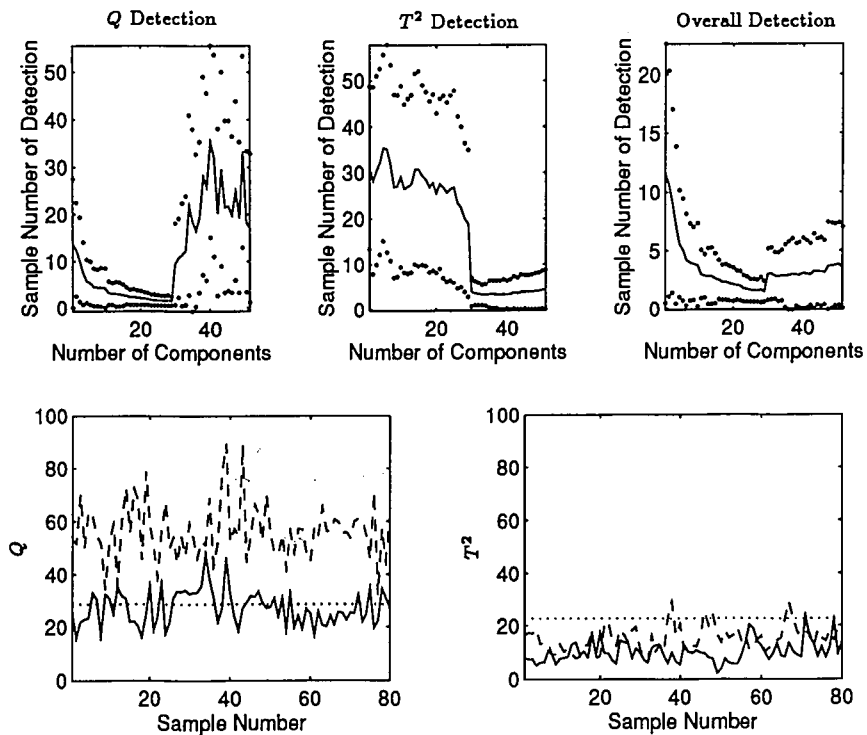


Figure 2.10: Top plots: Speed of Detection for Tennessee Eastman Disturbance 4 at 50% Magnitude Reduction versus Number of Components in the PCA Model. Bottom plots: Q and T^2 Monitoring Plots for Reduced Magnitude Disturbance 4 (solid line) and Disturbance 4 (dashed line). (sampling interval = 3 minutes).

2.3. DISTURBANCE ISOLATION

a 1 component model, but for this case the delay was approximately 15 minutes (5 samples). The lower two monitoring plots in Figure 2.9 demonstrate the increased difficulty in detecting smaller disturbances. The full magnitude disturbance is represented by the dashed line, the reduced magnitude by the solid line. This is especially visible from the Q chart which shows the statistic closely following the 95% confidence limit. These two plots were based on a model size of 13. Only samples occurring after the disturbance introduction were plotted.

Figure 2.10 shows the results of this analysis for disturbance 4 at 50% of its original magnitude. The speed of detection trends for the reduced magnitude case were much more dramatic than those observed for the full magnitude case (see Figure 2.7). Clearly the one or two component model was inappropriate for detection of the reduced magnitude disturbance 4. Detection by models of this size averaged at least 35 minutes after the detection by the model with 29 components. The lower two monitoring charts were provided to indicate the difficulty involved in detecting this reduced magnitude case even with a model with the most approximate number of components.

Similar results were observed for the remaining reduced magnitude disturbances. Models based on only one or two components tended to detect significantly later than the other models. Models of approximate size 30 or greater detected the fastest and with the least variance in sample of detection. In general, these results indicate that the PRESS statistic came closer than parallel analysis in choosing a model size having the best detection performance. This conclusion is consistent with the one presented in the previously published study by Himes et al. [6].

The plots for all reduced magnitude disturbances as well as the full magnitude cases are available in Appendix B.

2.3 Disturbance Isolation

It could be stated that the main goal of SPC is process improvement. This is to be achieved through a four step process. First, an empirical model is developed based on the normal operating conditions of the process. Second, the model is used to monitor

CHAPTER 2. CHOOSING APPROPRIATELY SIZED PCA MODELS

the process in an attempt to detect occurrences of abnormal operating conditions or disturbances, ie. departures from the model, greater than normal process variation. Next, the causes of the disturbances are determined. This is called isolation. Finally, a process changes might be implemented which would reduce the effects of the disturbances or eliminate the causes of the disturbances.

Once a new disturbance is detected, engineering knowledge and insight into the process is required to identify the cause of the disturbance. This can be a time consuming off-line procedure. It is assumed that each disturbance has a distinct characteristic effect on the process. Thus, the disturbance effect can be modeled. New disturbance data can then be compared on-line to the known disturbance models in an attempt to identify the cause immediately. There are two approaches to the on-line isolation: empirical and numerical. These approaches will be described in the following two sections.

2.3.1 Empirical Approach

Successful disturbance detection and isolation results using only the first two or three principal components have been presented in recent publications [12, 13, 17]. The advantage of this is that two-dimensional scatter plots can be made for the first component versus the second, and for either component versus the sum of squared residuals. Detection is easily observed graphically by a violation of either of the two control limits, T^2 and Q .

The expectation is that the disturbance will show a distinct trajectory as it violates the control limits, due to the fact that each disturbance disrupts the system differently. Future disturbances can be isolated by comparing and matching their trajectory to that of a set of known disturbances. If the new trajectory has no match this indicates the detection of a new type of disturbance whose cause should be investigated. Examples of these scatter plots for the TE disturbances 1, 4, and the reduced magnitude (RM) disturbance 1 are presented in Figure 2.11. The first 100 samples of simulation are plotted where the disturbance enters at sample 20. The top plots are scatter plot equivalents of the Q chart. The height of the dashed

2.3. DISTURBANCE ISOLATION

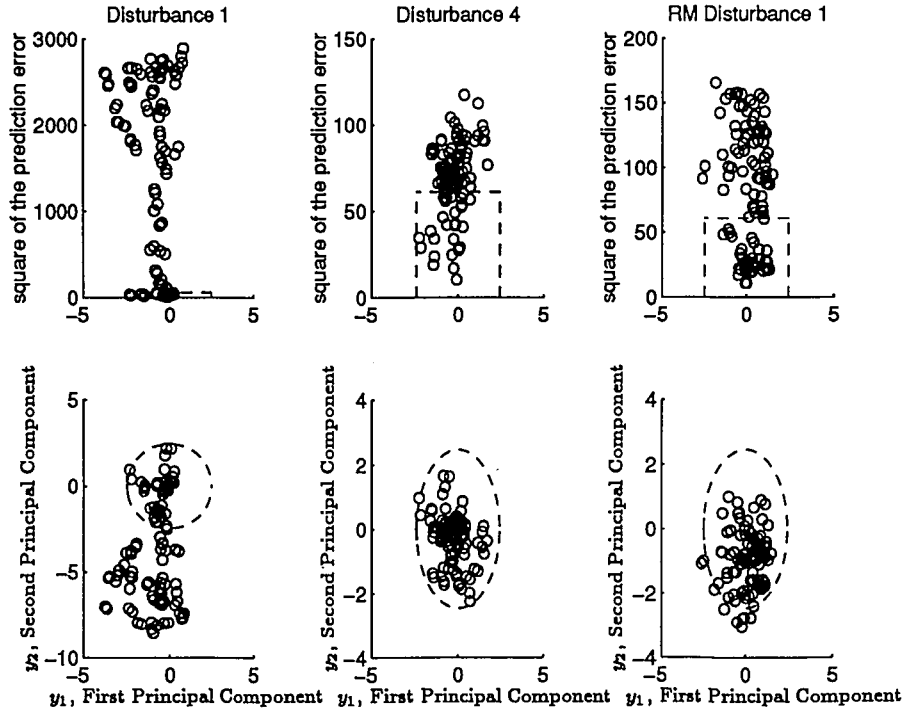


Figure 2.11: Disturbance Detection and Isolation Plots for Tennessee Eastman Disturbances 1 (left), 4 (middle), and reduced magnitude 1 (right).

box represents the Q control limit. The bottom plots are equivalents of the T^2 chart. The dashed oval is called a T^2 control limit ellipse.

One of the disadvantages of this technique for isolation is that it is graphical, not numerical. The practitioner must visually match trajectories that may appear similar. Consider the reduced magnitude results in the third column of Figure 2.11. These results are visually very similar to disturbance 4 (middle column) and could lead to an error by identifying this disturbance as disturbance 4 and not disturbance 1, as it is.

Another disadvantage of this technique is that if model size is an important factor in disturbance detection then scatter plots must be made for each combination of principal component pairs. Consequently the method loses its attractiveness once it becomes necessary for the model to have more than two principal components. Both

CHAPTER 2. CHOOSING APPROPRIATELY SIZED PCA MODELS

of these disadvantages can be avoided by utilizing a numerical approach developed by Ku et al. [14, 15]. This approach will be explained in the following section.

2.3.2 Numerical Approach

The numerical approach to disturbance isolation requires the development of a library of models based on disturbance data, each known disturbance having its own model. After a detection occurs during process monitoring, the subsequent samples can be projected onto each disturbance model in the library. If the new samples violate the control limits for a disturbance model then that disturbance can be rejected as a possibility. If the control limits are not violated for a particular disturbance model then it is possible that the new samples can be identified as similar to that disturbance. If no match is made with any of the available disturbance models in the library then it is possible that a new disturbance has been discovered.

The development of a disturbance model is the same as that for the monitoring model for normal operating conditions. The respective PCA model is given by Equation 1.7. The determination of the appropriate model size can be more difficult, however, due to the disturbance. On-set of a step disturbance causes the means of the process variables to shift. PCA, however, is a static method and will only rely on the mean of the samples used in the model development. Thus, PCA sees the disturbance transition as a period of increased process variation. The effect is a re-orientation of the loading vectors, the initial components explaining a greater amount of variance. The total amount of variance to explain, however, remains bounded due to auto-scaling. The result is that the remaining components explain less variance.

Figure 2.12 presents two parallel analysis plots for TE disturbance 1, one each for a 100 sample model and a 1000 sample model. Most of the samples in the 100 sample model are representative of the process transition whereas most of the samples in the 1000 sample model are representative of a new steady state. These plots demonstrate that the above two model types will be very different. The loading

2.3. DISTURBANCE ISOLATION

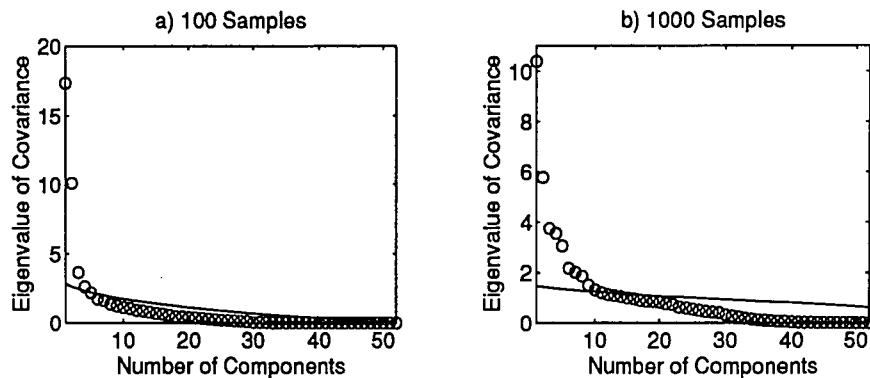


Figure 2.12: Parallel Analysis for the Tennessee Eastman Process, Disturbance Conditions. a) 100 Samples, b) 1000 Samples

vectors will be oriented differently and the number of significant principal components vary depending on the samples. The mainly transition-data model (100 sample) will represent the most highly dynamic data. Parallel analysis indicates that 4 components should be retained. The new-steady-state model is not really a disturbance model. It will most likely resemble the original-steady-state model, albeit with some different measurement variances and loadings because it is at a different state. This is supported by parallel analysis indicates that 10 components should be retained, coming close to the normal operating conditions value of 13. The difference is possibly due to the inclusion of transition data in the model.

There is good reason to believe that parallel analysis is unreliable for the transition data. TE disturbance 1 is a compositional step change. None of the controllers failed with this disturbance, so the number of relations remained the same. Additionally, unless this disturbance changed the number of reaction relationships, it is unlikely that the number of physical/chemical changed either. If this was true, then the actual number of components to retain for the model should also remain the same as for the normal operating condition model.

A model including both data types but dominated by steady state data may not properly identify a disturbance if the test data is from a transitional state. Figure 2.13 clearly demonstrates this situation for TE disturbance 1. The disturbance

CHAPTER 2. CHOOSING APPROPRIATELY SIZED PCA MODELS

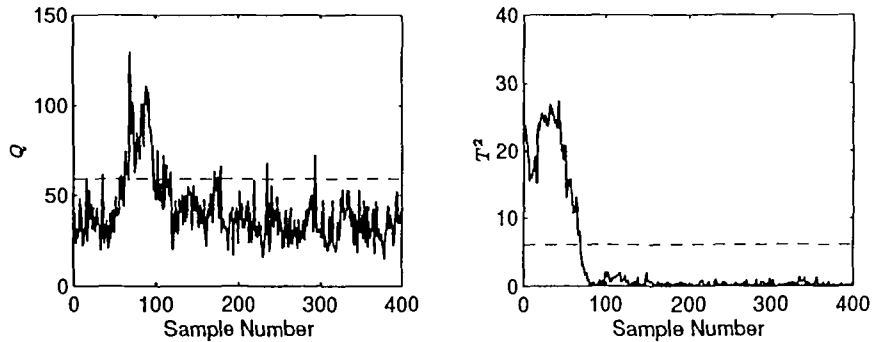


Figure 2.13: Isolation Plots for Disturbance 1 Data Projected Against the New-Steady-State Disturbance 1 Model

model was based on 1000 samples and two principal components, even though parallel analysis indicated that at least nine principal components were needed (see Figure 2.12). This made it essentially a new-steady-state model despite the inclusion of approximately 100 transition state samples. The T^2 statistic clearly did not isolate the initial (transition) samples and the Q statistic also had problems isolating. Only after 100+ samples, a little over five hours, after the start of the isolation procedure was the disturbance isolated. The reason for this is that the new steady state was reached and thus the new data matched the model.

Examples of the numerical isolation procedure for disturbances 1, 4, and 1 at reduced magnitude are presented in the following Figures. Each disturbance model was based on 100 samples of transitory data. Each had a model size of 2 principal components for comparison with the empirical approach. And each Figure contains three pairs of plots. The top pair of plots in Figure 2.14, for example, represent the projection of disturbance 1 data onto a disturbance 1 model. The middle pair of plots represent the projection of disturbance 1 data onto a disturbance 4 model. And the bottom pair of plots are for projection of disturbance 1 data onto a model for reduced magnitude disturbance 1. The plots in Figures 2.15 and 2.16 are based respectively on the projections of disturbance 4 data and reduced disturbance 1 data onto each of the disturbance models.

Based on Figure 2.14, it is clear that data for disturbance 1 was easily isolated

2.3. DISTURBANCE ISOLATION

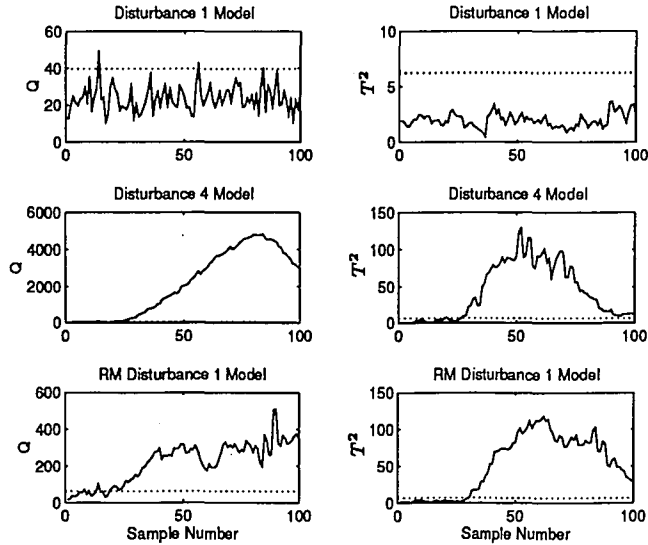


Figure 2.14: Isolation Plots for a Disturbance 1 Data Projected onto a Disturbance 1 Model (top), a Disturbance 4 Model (middle), and a Reduced Magnitude Disturbance 1 Model (bottom).

by the disturbance 1 model and rejected by the other two models. This is consistent with the empirical results in Figure 2.11. The fact that the reduced magnitude model rejected the full magnitude disturbance may be an indication of a flawed method. One reason for the mismatch is that the reduced magnitude case reached its new steady state much faster. Ku et al. [15] has shown that the full magnitude disturbance 1 reaches its new steady state in about five hours. The 100 samples included in the reduced magnitude model probably contained too many steady state samples to be an effective transition model. However, a model based on only 20 samples of transition data may not make a very good model either. In this case, a model bank of steady states might have been more appropriate. Another possible reason for the mismatch is that the full magnitude disturbance caused greater variation of process variables and may have caused the control structure to react differently than what occurred for the reduced case. If this was the case, a non-linear PCA method such as that presented by Trevor Hastie and Werner Stuetzle [5] might be warranted.

CHAPTER 2. CHOOSING APPROPRIATELY SIZED PCA MODELS

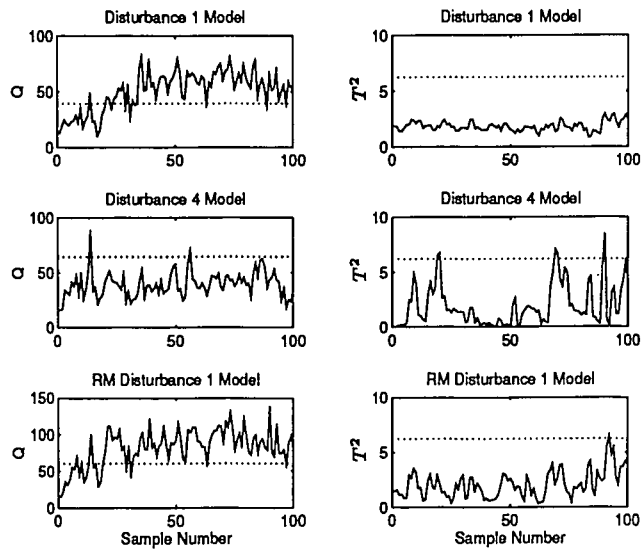


Figure 2.15: Isolation Plots for a Disturbance 4 Data Projected onto a Disturbance 1 Model (top), a Disturbance 4 Model (middle), and a Reduced Magnitude Disturbance 1 Model (bottom).

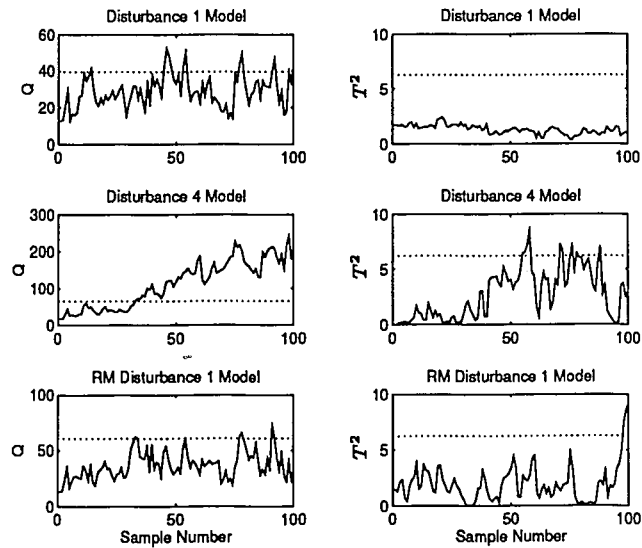


Figure 2.16: Isolation Plots for Reduced Magnitude Disturbance 1 Data Projected onto a Disturbance 1 Model (top), a Disturbance 4 Model (middle), and a Reduced Magnitude Disturbance 1 Model (bottom).

2.4. SUMMARY

The results presented in Figures 2.15 and 2.16 are not consistent with the empirical results. Figure 2.15 clearly demonstrates that disturbance 4 data is isolated by the disturbance 4 model but is rejected by the other two models. It was pointed out that the empirical result might have difficulty isolating disturbance 4 from reduced magnitude disturbance 1. Figure 2.16 supports the result of Figure 2.15. Reduced magnitude disturbance 1 is not confused with disturbance 4. It also shows that this data is isolated with the disturbance 1 model, indicating that the variables do move in a similar fashion.

2.4 Summary

This chapter began with a review of several methods which could be used for the selection of a principal component model size. It was shown that these different methods could give very different results, an unfortunate reality well documented in the literature [10]. But it was reasoned that parallel analysis and the PRESS statistic indicated lower and upper bounds, respectively, for the number of principal components to be used in a PCA model for the TE process. This left a large number of possible model sizes to consider. In addition, it was noted that recent publications have presented positive results utilizing only the first few components for a model [12, 13, 17]. The key question resulting from these issues was: How sensitive is disturbance detection and isolation to model size?

Section 2.2 presented an investigation into the sensitivity of detection to model size. It was found that for large disturbances there was very little sensitivity, with only the slightest improvement with larger-sized models. The largest detection delay between model sizes was on the order of six minutes. For smaller disturbances, however, the sensitivity was much more pronounced. Larger sized models clearly performed better than two component models. Detection differences were observed at as much as 35 minutes! In addition, it could be argued that PCA was not necessary at all for TE monitoring. The detection trends indicated that a model utilizing all 52 components would also have provided excellent detection. This result might suggest that the Tennessee Eastman simulation is an atypical problem for

CHAPTER 2. CHOOSING APPROPRIATELY SIZED PCA MODELS

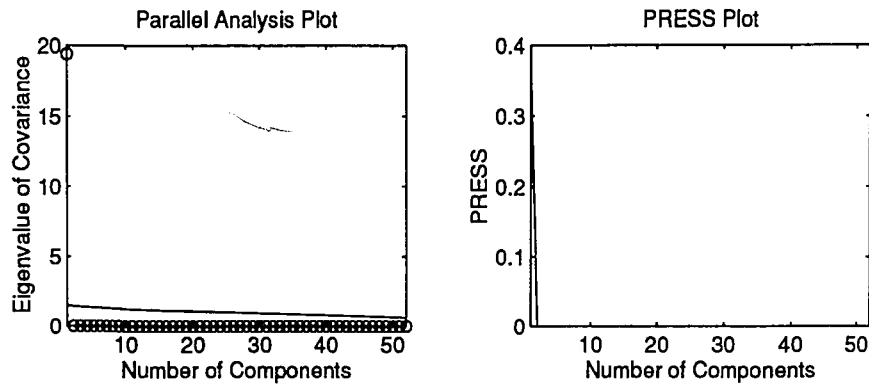


Figure 2.17: Parallel Analysis and Cross-Validation for Data Scaled by Measurement Span

SPC.

These results make a strong contrast with the published results based on two or three component models. This inconsistency may be due to several differences between the PCA process presented here and that used elsewhere [12, 13, 17]. The first difference is method of scaling. If the TE data were scaled by measurement spans instead of auto-scaling, parallel analysis and cross-validation would both indicate a one component model (see Figure 2.17). Another difference is that many SPC practitioners use the method of Partial Least Squares, a variation on PCA. In addition, many of the published examples are based on a single process unit as opposed to the TE process which comprises five units. And finally, magnitude of disturbance is also a critical issue in detection. The larger a disturbance is, the easier it will be detected.

If the only SPC issue of interest were quick and accurate detection, then the results indicated by this study would suggest that only the T^2 calculation would be necessary. But this is not the case. Isolation of the disturbance is an equally important issue. The separation of the collinearity and noise from the inherent information may provide additional insight into the process and the disturbance. It was reasoned in Subsection 2.1.3 that many of the collinear relations are related to the linear control structure of the process. By monitoring both the T^2 and Q

2.4. SUMMARY

statistics it may be possible to infer if the inherent variation is out of control (T^2) or if the constraining relations have changed (Q). This is especially true once a new steady state is reached. At this state, controller action may or may not have brought measurements close to their original variations and inherent variation back into control. The constraining relations, however, would most likely be different due to new secondary controller setpoints in the cascade loops and shifts in mean values of measurements, especially valve positions.

Section 2.3 highlighted the advantages and disadvantages between empirical and numerical isolation techniques. The most important advantage to the numerical approach is the establishment of a quantitative criterion for isolation rather than a visual one. Unfortunately, development of appropriate PCA models for disturbance data can be more difficult than for a base model. These models might be statistically inferior due to lack of sufficient transition data samples. In addition, the methods of choosing model size all indicate that only the first few components are necessary for the disturbance model. It was reasoned that this can be due to the influence of increased process variation and most likely not due to a reduction in the number of constraining relations.

Since a sensitivity study such as that presented in Section 2.2 would not be possible to employ in an industrial setting, the PCA practitioner must rely on the methods available for choosing an appropriate model size as well as some intuition into the process. However, balancing the various methods of choosing, the sensitivity study, and the advantage of using two monitoring charts, a PCA model size of about 30 components seems appropriate for SPC of the Tennessee Eastman process under normal operating conditions. This model size will provide the fastest possible detection without sacrificing the isolation benefits provided using both the T^2 and Q statistics.

CHAPTER 2. CHOOSING APPROPRIATELY SIZED PCA MODELS

Chapter 3

Decentralized PCA Models in Multivariate SPC

3.1 Decentralized PCA Method

In Chapter 2 and in work by Ku et. al. [15] centralized PCA models were used for disturbance detection and isolation. The term centralized refers to the fact that all TE variables were utilized in the formation of a single model. This model was shown to be quite effective in disturbance detection and isolation. But the Q and T^2 monitoring charts yield little information about what had occurred in the process beyond the onset of a disturbance and the possible return to steady state.

Valuable insights into the process might be obtained through the decentralized method, that is, the development of a PCA model for each individual operation unit in the process. A similar method for PLS is described by MacGregor et al. [17]. It is logical to expect that the process unit in which a disturbance originated would go out of control before the other units. This would be an aid since a root cause investigation could focus around a single unit instead of a whole plant. Additionally, it would be possible to observe any propagation of the disturbance throughout the plant, thereby evaluating the effectiveness of the control structure.

TE is an ideal case study for the decentralized method in that the process includes five operation units: a two phase reaction vessel, a condenser, a separator, a recycle compressor, and a stripper. For the purposes of decentralized PCA, these outputs were combined into five models. Each of the unit models was mainly comprised of the variables which are direct measurements for that unit. Measurements applying to connecting streams between units were included in the models for both units. For an example, the stream from the reactor to the condenser was assumed to have the same temperature and pressure as the reactor, thus these variables were common to both the reactor and condenser. The division of variables into their decentralized units is presented in Table 3.1. In addition, this study included a model for product quality. This fictitious "unit" was comprised solely of the composition measurements (measurement numbers 37-41) of the product stream.

3.2 Applications

3.2.1 Local Disturbance Compensation

As an initial demonstration of the decentralized method, consider TE disturbance #4 (D4). This is a step change to the reactor cooling water inlet temperature. Figure 3.1 presents the Q and T^2 control charts for centralized monitoring through plant wide SPC charts. The Q chart indicates the on-set of a disturbance at hour one somewhere in the plant and the quick attainment of a new steady state. The T^2 chart did not detect the disturbance at hour one but shows five hours of apparent normal variation, which includes several false alarms between hours two and three. Investigation of the individual components and/or measurements would be needed to further isolate the cause of the disturbance.

The decentralized method is represented in Figure 3.2. The Q and T^2 control charts are shown for each of the five units and for product quality. Control limits based on 95 and 99% type I error risk are plotted as dashed lines in both charts. A circle indicates the sample that is first to violate the 95% control limits after the initiation of the disturbance. The time of this detection is provided beneath each

3.2. APPLICATIONS

Table 3.1: Division of Process Variables into Decentralized Units

#	Measurement	Condenser	Compressor	Reactor	Stripper	Separator
1	A Feed Flow (stream 1)			x		
2	D Feed Flow (stream 2)			x		
3	E Feed Flow (stream 3)			x		
4	A and C Feed Flow (stream 4)				x	
5	Recycle Flow (stream 8)		x	x		
6	Reactor Feed Rate (stream 6)		x	x		
7	Reactor Pressure	x	x	x		
8	Reactor Level			x		
9	Reactor Temperature	x		x		
10	Purge Rate (stream 9)		x			x
11	Product Separator Temperature	x	x		x	x
12	Product Separator Level					x
13	Product Separator Pressure		x			x
14	Product Separator Underflow				x	x
15	Stripper Level				x	
16	Stripper Pressure		x	x	x	
17	Stripper Underflow (stream 11)				x	
18	Stripper Temperature		x		x	
19	Stripper Steam Flow				x	
20	Compressor Work		x			
21	Reactor CWR Temperature			x		
22	Condenser CWR Temperature	x				
23-28	Component Analysis (stream 6)			x		
29-36	Component Analysis (stream 9)		x			x
37-41	Component Analysis (stream 11)				x	
42	D Feed Valve (stream 1)			x		
43	E Feed Valve (stream 2)			x		
44	A Feed Valve (stream 3)			x		
45	A and C Feed Valve (stream 4)				x	
46	Compressor Recycle Valve		x			
47	Purge Valve (stream 9)		x			x
48	Separator Underflow Valve				x	x
49	Stripper Underflow Valve				x	
50	Stripper Steam Valve				x	
51	Reactor CWR Valve			x		
52	Condenser CWR Valve	x				

CHAPTER 3. DECENTRALIZED PCA MODELS IN MULTIVARIATE SPC

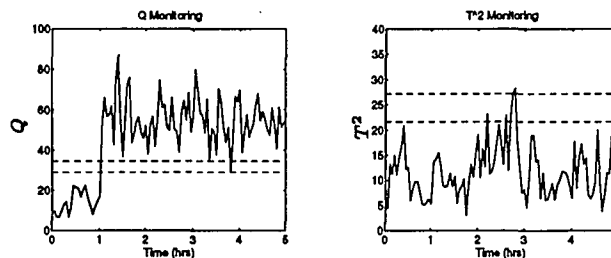


Figure 3.1: Centralized Monitoring of TE Disturbance 4, Reactor Cooling Water Inlet Temperature Step Change

chart.

It is clear from these plots that the reactor quickly went out of statistical control. All other units remained in statistical control and product quality was unaffected. Efforts to isolate the cause could immediately be focused around the reactor variables, a reduction from 52 to 20 variables. This is an example of local compensation of the disturbance. By this it is meant that the control structure associated with the reactor was able to compensate for the majority of the disturbance. In addition, the fact that the disturbance failed to propagate to other units indicates that the control structure was well designed for handling D4.

As a second example, consider TE disturbance #5 (D5), a positive step change in the condenser cooling water inlet temperature. The decentralized charts for this case are presented in Figure 3.3. The charts show that the control structure was incapable of preventing the disturbance from propagating through the plant. This was not surprising. In order to compensate for this disturbance, the cooling water valve must open, see Figure 1.1. With this control structure the appropriate action could not occur until a change in the stripper product flow rate was detected. Fortunately, this occurred quickly. A possible control structure improvement would make use of the condenser cooling water outlet temperature, an available but unused measurement. This alternate control structure might have eliminated the disturbance propagation.

If this disturbance was not known it would not be possible to determine from these charts which unit was affected first by the disturbance. Detection occurs on either T^2 or Q , whichever chart is first. Thus, detection was immediate in all units,

3.2. APPLICATIONS

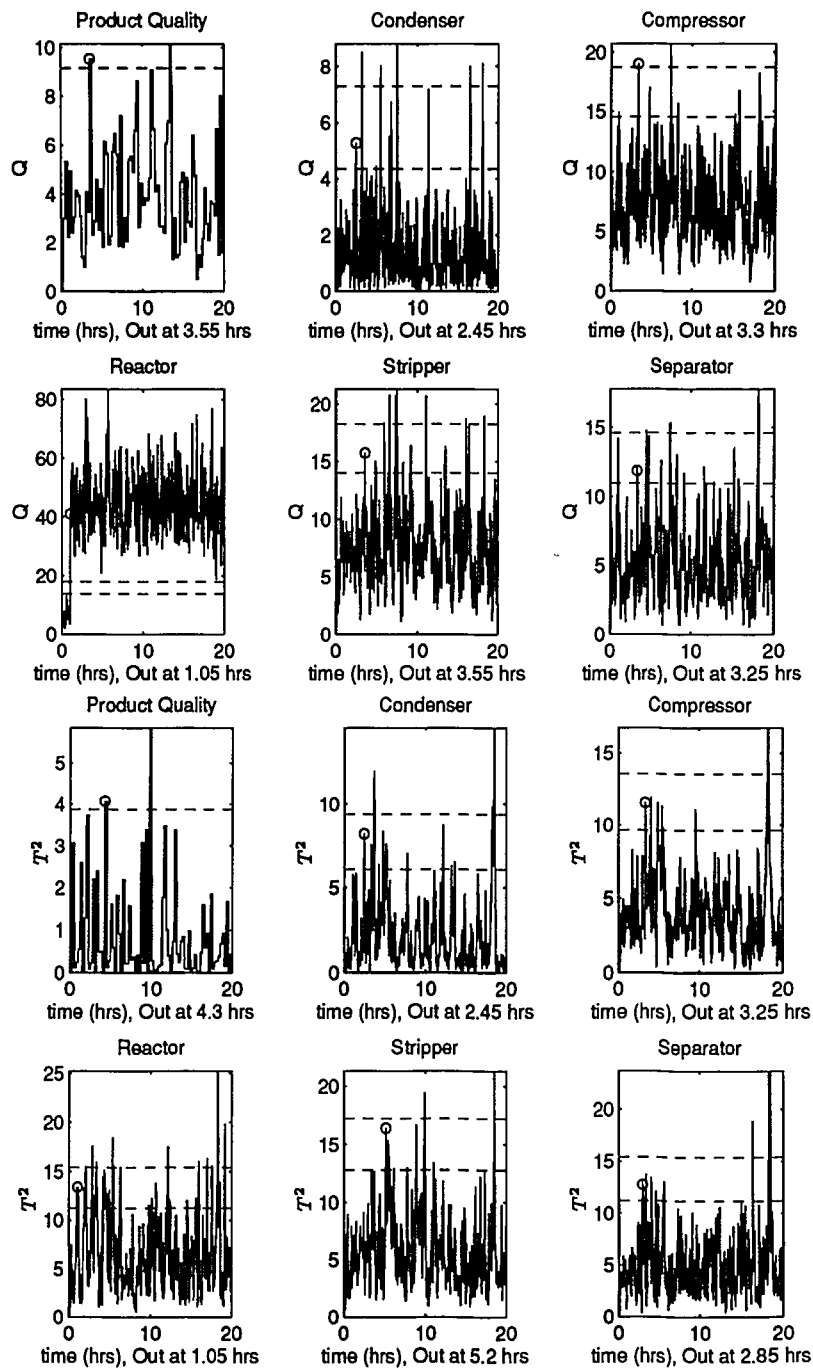


Figure 3.2: Decentralized Monitoring of TE Disturbance #4, Reactor Cooling Water Inlet Temperature Step Change

CHAPTER 3. DECENTRALIZED PCA MODELS IN MULTIVARIATE SPC

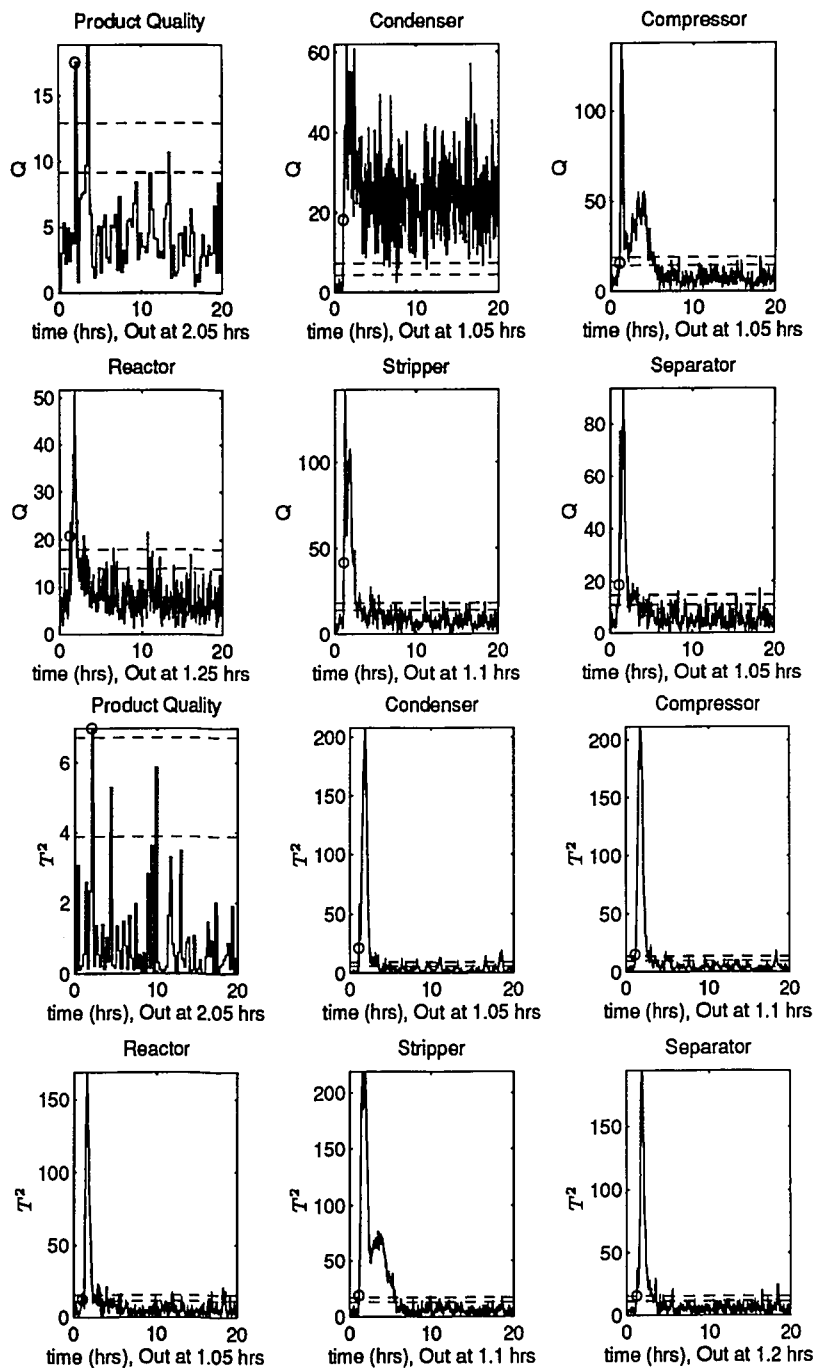


Figure 3.3: Decentralized Monitoring of TE Disturbance #5, Condenser Cooling Water Inlet Temperature Step Change

3.2. APPLICATIONS

having occurred within one to two minutes of each other. Additional simulations using different random seeds indicated that this time difference was not significant. Part of the reason for this fast plant-wide upset is that the stripper liquid flow rate measurement was used for adjusting the condenser cooling water valve. The delay in measuring the effect of the disturbance by the stripper liquid flow caused a delay in its compensation. In the meantime, changes in plant-wide temperatures and pressures upset all units, and initiated plant-wide control action.

By ten hours the plant reached a new steady state. All the decentralized control charts, except for the Q chart of the condenser, show that the units returned to statistical process control. This indicates that the control structure associated with the condenser might have been responsible for the major action in disturbance compensation. Analysis of the condenser variables confirmed that only the cooling water valve position average value had been shifted by the disturbance.

3.2.2 Distributed Disturbance Compensation

Local compensation for a disturbance is not always possible. The disturbance magnitude might overwhelm the local control structure or corrective action might only be possible via intervention of another unit. An example of this situation can be demonstrated with TE disturbance #6 (D6), loss of component A feed stream 1. The only remaining supply of component A entered the process through stripper feed stream. Unfortunately, this stream did not contain the stoichiometric ratio of A to C needed for complete consumption of C in the reactor. Therefore, excess C was purged and the production rate was dropped. The SPC result was that compensation for the disturbance was distributed among all units.

Figure 3.4 presents the results for this disturbance. The disturbance propagation is clearly evident on all charts. Even at 20 hours, the plant continued to go further out of statistical control in an effort to compensate for this disturbance. Detection on the Reactor Q chart occurred 12 minutes before detection on any other chart, correctly indicating that the D6 was initiated in the reactor.

As a second example of distributed compensation, consider TE disturbance #1

CHAPTER 3. DECENTRALIZED PCA MODELS IN MULTIVARIATE SPC

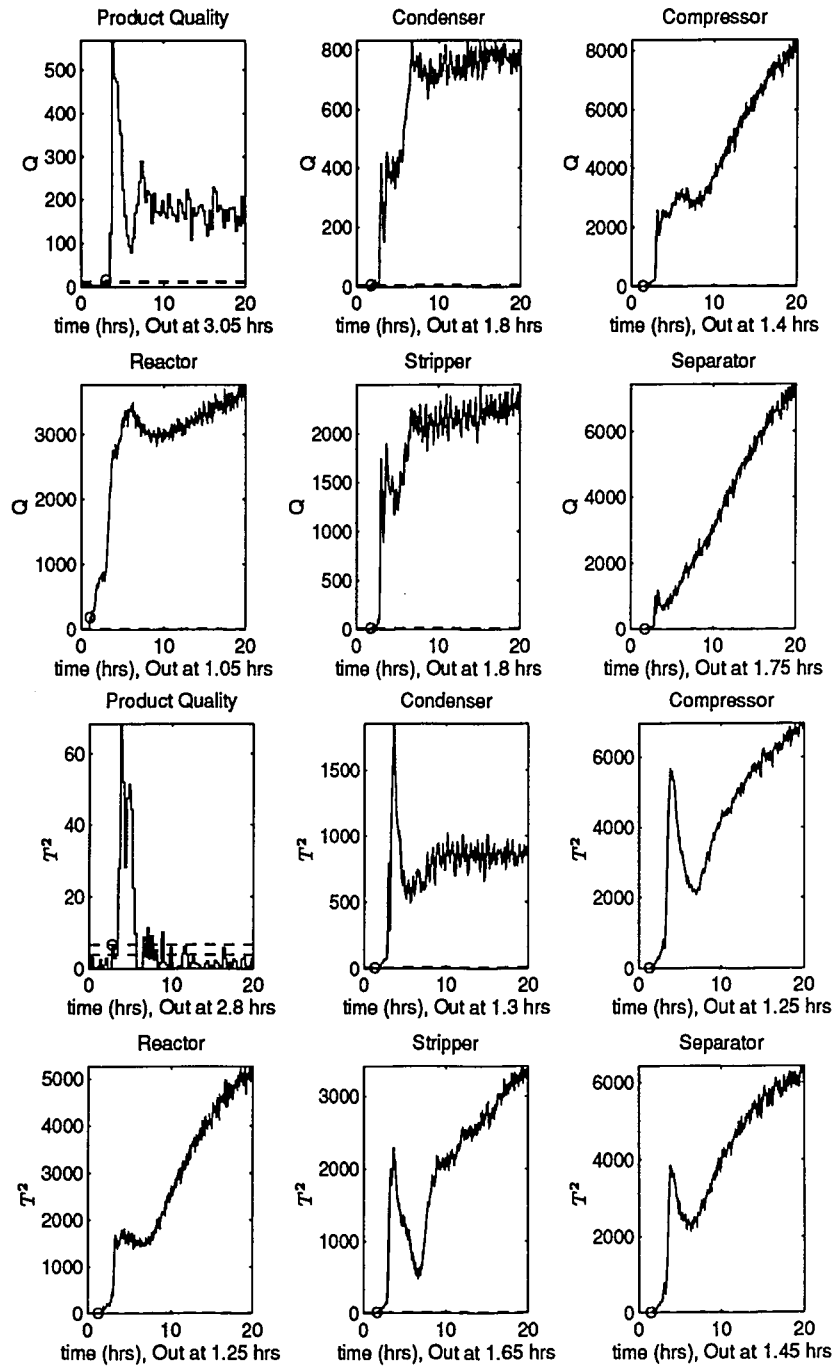


Figure 3.4: Decentralized Monitoring of TE Disturbance #6, A Feed Loss (Stream 1)

3.2. APPLICATIONS

(D1), a composition step change in the stripper feed. Local compensation was clearly impossible since only the reactor feed streams could have adjusted for the composition change. The results for D1 are plotted in Figure 3.5. Although not all of the charts went out of control simultaneously, many were close, making it difficult to determine the unit of disturbance initiation. The disturbance quickly propagated throughout the plant and eventually a new steady state was reached. Interestingly, some of the charts returned to statistical control, indicating that disturbance compensation no longer made use of the local control structure of these units.

3.2.3 Reduced Magnitude Disturbances

An initial hypothesis was that the unit first subjected to the disturbance would also first detect the disturbance and that the propagation could be followed throughout the process. This was motivated, in part, by research conducted by MacGregor et al. [17] in which a multisection tubular reactor producing LDPE was monitored using an approach similar to the decentralized technique presented here. Unfortunately, it was difficult to verify this hypothesis for the TE process. Part of the problem was that the TE process exists principally in the gas phase. Temperature and pressure changes quickly propagated throughout, especially since the TE disturbances were large in magnitude. Thus, the analysis was repeated with smaller disturbances which might result in increased resolution between charts.

Figure 3.6 shows the results for D1 at 20% of its original magnitude. The most significant change between the two D1 cases was that the reduced magnitude disturbance was not detectable on either the product quality or the condenser charts, eliminating their units from fault diagnosis consideration. The other reduced magnitude D1 charts still went out of control too closely to indicate the unit of disturbance initiation. In addition, it was difficult to discern whether or not the first detection was a false or a real alarm. For example, the stripper Q chart went out of control at 1.6 hours but then returned to control for a while before it went out again about an hour later. This uncertainty may be a severe limitation for this aspect of the

CHAPTER 3. DECENTRALIZED PCA MODELS IN MULTIVARIATE SPC

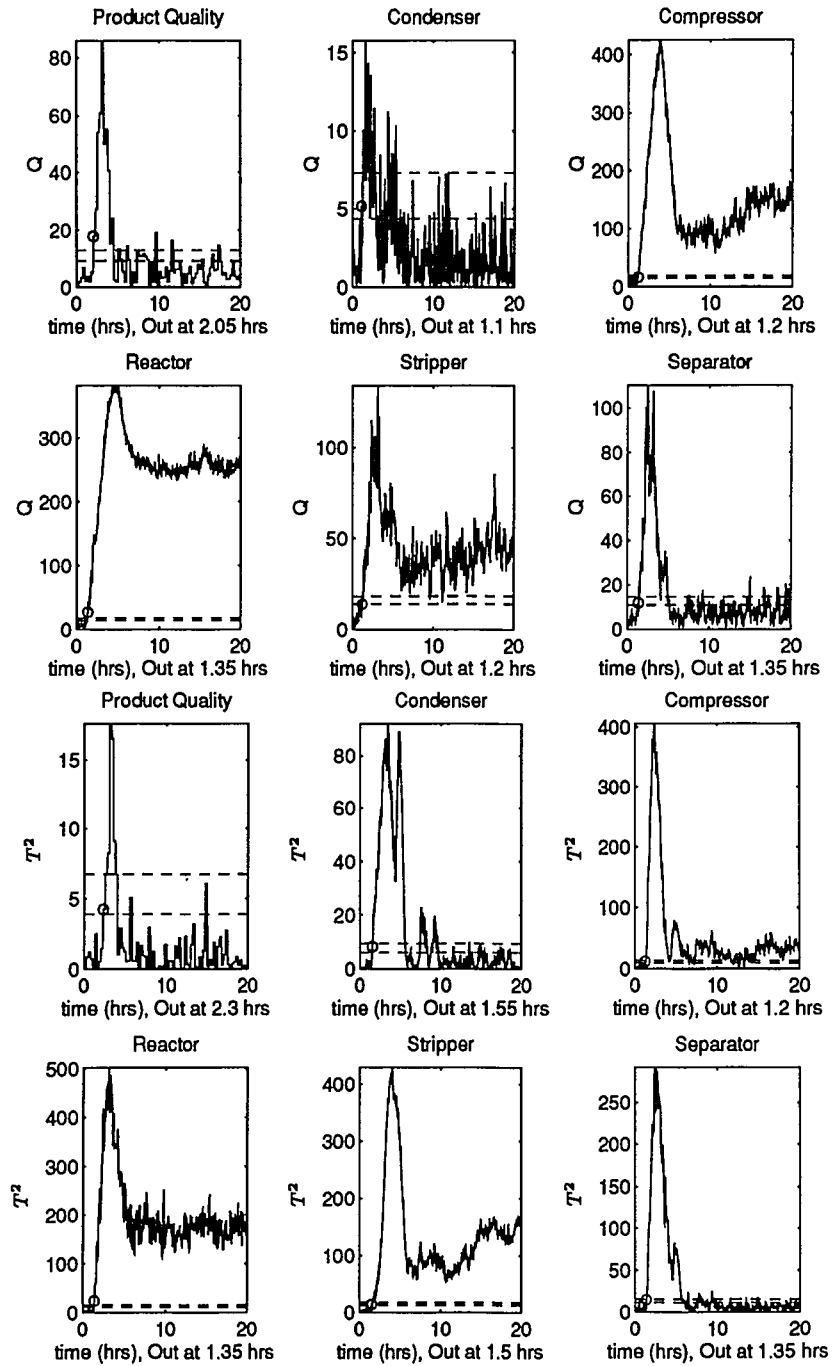


Figure 3.5: Decentralized Monitoring of TE Disturbance #1, Composition Step Change (Stream 4)

3.2. APPLICATIONS

decentralized procedure in an industrial application.

3.2.4 Control Structure Evaluation

The evaluation of the control structure might be possible through observation of any disturbance propagations throughout the plant. These observations might, in turn, suggest possible modifications for control structure improvements. In Subsection 3.2.1, the use of the condenser cooling water outlet temperature measurement was suggested as one possible improvement.

Although many control structure changes would be possible, it was decided to replace the PI loop, which manipulated the condenser cooling water return valve, with a cascade loop. In this new loop, the condenser cooling water outlet temperature was used as the slave variable and the product flowrate was used as the master. This new structure was found to perform excellently with respect to D5 by preventing any propagation to occur. Even TE disturbance #7 (D7), header pressure loss, failed to propagate under the new structure and the condenser unit came closer to remaining in statistical control for the other disturbances.

Unfortunately, the new structure did cause some problems. Simulation of D1 nearly shut down and D6 did shut down due to excessive reactor pressure. The strict control on the condenser coolant removed some of the flexibility the original structure had to compensate for these disturbances. Additionally, the new structure increased the steady state variation of nearly all the process variables. The only reduction was the condenser cooling water outlet temperature. This result was the exact opposite of one of SPC's goals, namely the elimination of sources of process variation. Thus, the benefits of this new structure for the TE process are doubtful; but the benefits of decentralized monitoring as a tool for control structure evaluation are positive.

CHAPTER 3. DECENTRALIZED PCA MODELS IN MULTIVARIATE SPC

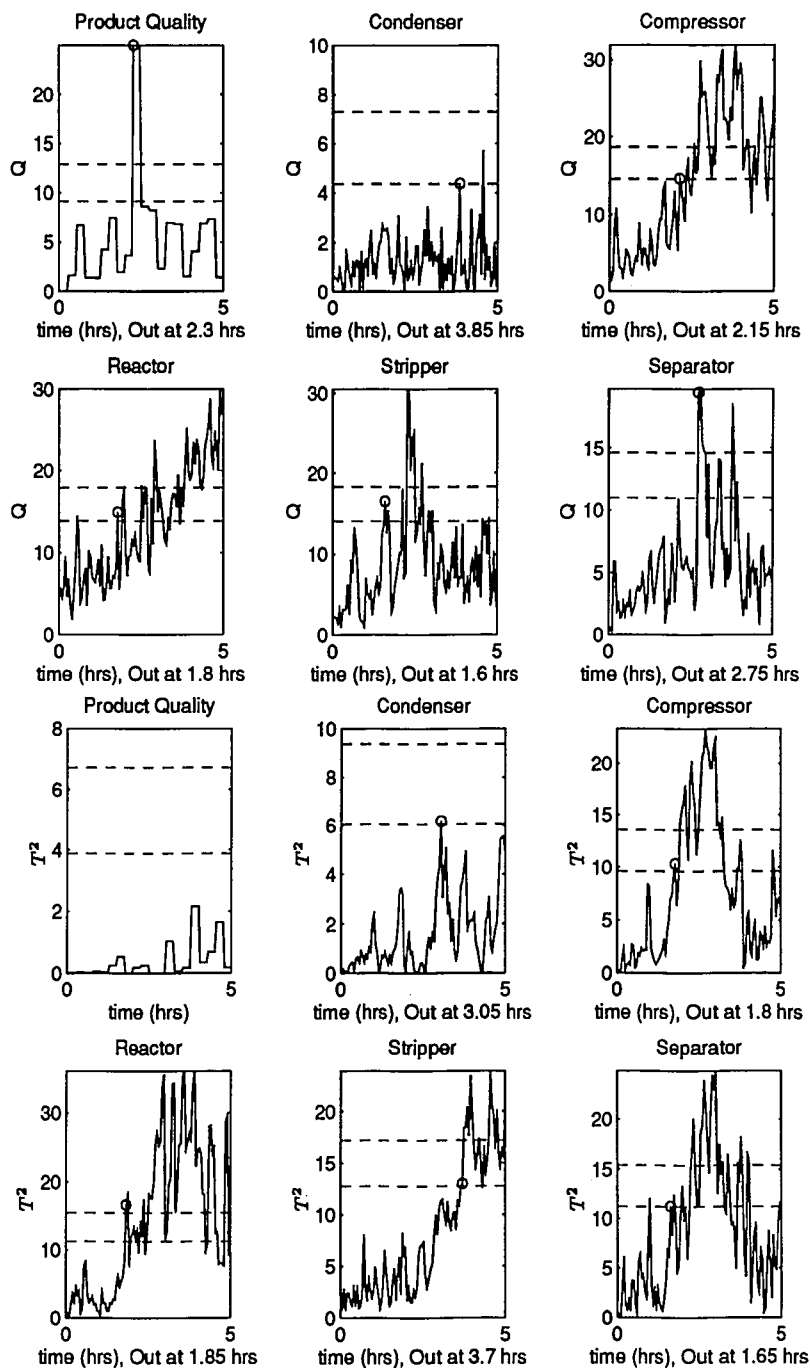


Figure 3.6: Decentralized Monitoring of TE Reduced Magnitude Disturbance #1, Composition Step Change (Stream 4)

3.3. SUMMARY

3.3 Summary

This chapter has shown examples of how decentralized monitoring of a process can be an additional tool in isolating a disturbance and evaluating the control structure. Although it was anticipated that the initial detection would be most useful for these purposes, it was found that a longer view of the process revealed more information. Specifically, isolation of a disturbance was most likely to occur by examining the unit(s) remaining out of statistical control once a new steady state had been reached. This is because initial detections tended to occur quickly on all charts due to the fast disturbance propagation possible in a gaseous plant. In addition, it was not always clear whether or not a detection was a real or a false alarm, thereby obscuring which chart detected first.

CHAPTER 3. DECENTRALIZED PCA MODELS IN MULTIVARIATE SPC

Bibliography

- [1] Raymond B. Cattell. The Scree Test for the Number of Factors. *Multivariate Behavioral Research*, 1:245-276, 1966.
- [2] J. J. Downs and E. F. Vogel. A Plant-Wide Industrial Process Control Problem. *Computers and Chemical Engineering*, 17(3):245-255, 1993.
- [3] H. T. Eastment and W. J. Krzanowski. Cross-Validatory Choice of the Number of Components from a Principal Component Analysis. *Technometrics*, 24(1):73-77, February 1982.
- [4] Paul Geladi and Bruce R. Kowalski. Partial Least-Squares Regression: A Tutorial. *Analytica Chimica Acta*, 185:1-17, 1986.
- [5] Trevor Hastie and Werner Stuetzle. Principal Curves. *Journal of the American Statistical Association*, 84(406):502-516, 1989.
- [6] David M. Himes, Robert H. Storer, and Christos Georgakis. Determination of the Number of Principal Components for Disturbance Detection and Isolation. In *Proceeding of the 1994 American Control Conference*, pages 1279-1283, 1994.
- [7] John L. Horn. A Rationale and Test for the Number of Factors in Factor Analysis. *Psychometrika*, 30(2):179-185, June 1965.
- [8] Harold Hotelling. Analysis of a Complex of Statistical Variables into Principal Components. *Journal of Educational Psychology*, 24:417-441, 498-520, 1933.

BIBLIOGRAPHY

- [9] J. Edward Jackson. Quality Control Methods for Several Related Variables. *Technometrics*, 1(4), 1959.
- [10] J. Edward Jackson. *A User's Guide to Principal Components*. John Wiley & Sons, Inc., 1991.
- [11] J. Edward Jackson and Govind S. Mudholkar. Control Procedures for Residuals Associated with Principal Component Analysis. *Technometrics*, 21(3):341-349, August 1979.
- [12] Michael H. Kaspar and W. Harmon Ray. Chemometric Methods for Process Monitoring and High-Performance Controller Design. *AIChE Journal*, 38(10):1593-1608, October 1992.
- [13] James V. Kresta, John F. MacGregor, and Thomas E. Marlin. Multivariate Statistical Monitoring of Process Operating Performance. *The Canadian Journal of Chemical Engineering*, 69:35-47, February 1991.
- [14] Wenfu Ku, Robert H. Storer, and Christos Georgakis. Isolation of Disturbances in Statistical Process Control by Use of Approximate Models. Presented at the 1993 AIChE Annual Meeting, St. Louis, MO.
- [15] Wenfu Ku, Robert H. Storer, and Christos Georgakis. Uses of Principal Component Analysis for Disturbance Detection and Isolation. In *Proceedings of Computer Integrated Manufacturing in the Process Industries*, 1994.
- [16] Philip R. Lyman and Christos Georgakis. Plant-wide Control of the Tennessee Eastman Problem. *Computers and Chemical Engineering*, 19(3):321-331, 1995.
- [17] John F. MacGregor, Christiane Jaeckle, Costas Kiparissides, and M. Koutoudi. Process Monitoring and Diagnosis by Multiblock PLS Methods. *AIChE Journal*, 40(5):826-837, May 1994.
- [18] Randel M. Price, Philip R. Lyman, and Christos Georgakis. Throughput Manipulation in Plant-Wide Control Structures. *Ind. Eng. Chem. Res.* In Print.

BIBLIOGRAPHY

- [19] Randel M. Price, Philip R. Lyman, and Christos Georgakis. Selection of Throughput Manipulators for Plant-wide Control Structures. In *Proceedings of the Second European Control Conference*, pages 1060–1066. ECC, 1993. Groningen, The Netherlands, June 28-July 1 1993.
- [20] Barry M. Wise, N. L. Ricker, D. F. Veltkamp, and Bruce R. Kowalski. A Theoretical Basis for the Use of Principal Component Models for Monitoring Multivariate Processes. *Process Control and Quality*, 1:41–51, 1990.
- [21] Svante Wold. Cross-Validatory Estimation of the Number of Components in Factor and Principal Components Models. *Technometrics*, 20(4):397–405, November 1978.

BIBLIOGRAPHY

Appendix A

Nomenclature

f	fraction of censored data
k	size of PCA model
m	number of samples
n	number of variables
p	loading (principal axes) vector
t	score (principal component) vector
x	data vector, single data sample
y	scores (principal component) vector
D_k	degrees of freedom needed to fit k^{th} component
D_r	degrees of freedom remaining after k^{th} fit
EK	Eastment and Krzanowski cross validation statistic
P	loadings (principal axes) matrix
Q	sum of squared residuals
S	covariance matrix
T	scores (principal component) matrix
T^2	sum of squared principal components
U	left singular vectors matrix
V	right singular vectors matrix, eigenvector matrix
W	PCA model
X	data matrix

APPENDIX A. NOMENCLATURE

Y	scores (principal component) matrix
ϵ	residual
η	sample of detection number
Λ	eigenvalues of S
Σ	eigenvalues of X

Abbreviations

LDPE	Low Density Polyethylene
PCA	Principal Component Analysis
PRESS	Prediction Sum of Squares
SPC	Statistical Process Control
SVD	Singular Value Decomposition
TE	Tennessee Eastman

Appendix B

Speed of Detection

It was stated in Section 2.2.2 that the sensitivity of detection to model size was investigated for each of the TE step disturbances, except disturbances 3 and 9. The results for the all of the disturbances were not presented there in order to facilitate comprehension of the main points. In this appendix, the remaining disturbances are represented as further illustrations.

Each figure is comprised of a series of plots. In all plots, only samples collected after disturbance initiation are shown. The top three plots represent the speed of detection versus the number of components in the model, i. e. model size, for the full magnitude disturbance. The middle three plots represent the speed of detection versus the number of components for the reduced magnitude disturbances. Disturbances 1 and 6 are at 20% of the original magnitude, and disturbances 4, 5 and 7 are at 50% of the original. Disturbance 2 is activated at two locations in the encrypted simulation code, and at each location the effect is reduced to 20% of the original magnitude. The solid lines in these plots reflect the average number of samples occurring between disturbance initiation and detection. The dotted lines indicate the standard deviation in detection.

The bottom two plots are Q and T^2 monitoring plots with 95% confidence limits (dotted lines) and based on a PCA model of size 13. The solid lines represent the reduced magnitude data and the dashed lines represent the full magnitude data.

APPENDIX B. SPEED OF DETECTION

These monitoring plots demonstrate that, in general, the full magnitude disturbances cause large and immediate process upsets. Detection is simple and quick, with little or no sensitivity to model size. The reduced magnitude disturbances, however, take longer to upset the process significantly. Detection could be difficult since the monitoring trajectory may just barely violate the confidence limit. Detection of reduced magnitude disturbance 2 is so slow that its speed of detection average and standard deviation is nearly as bad as that for the no disturbance case (Figure 2.5). But all the overall detection plots seem to point to the same conclusion. Detection of any one disturbance is the fastest and with the least variance when the model size is large.

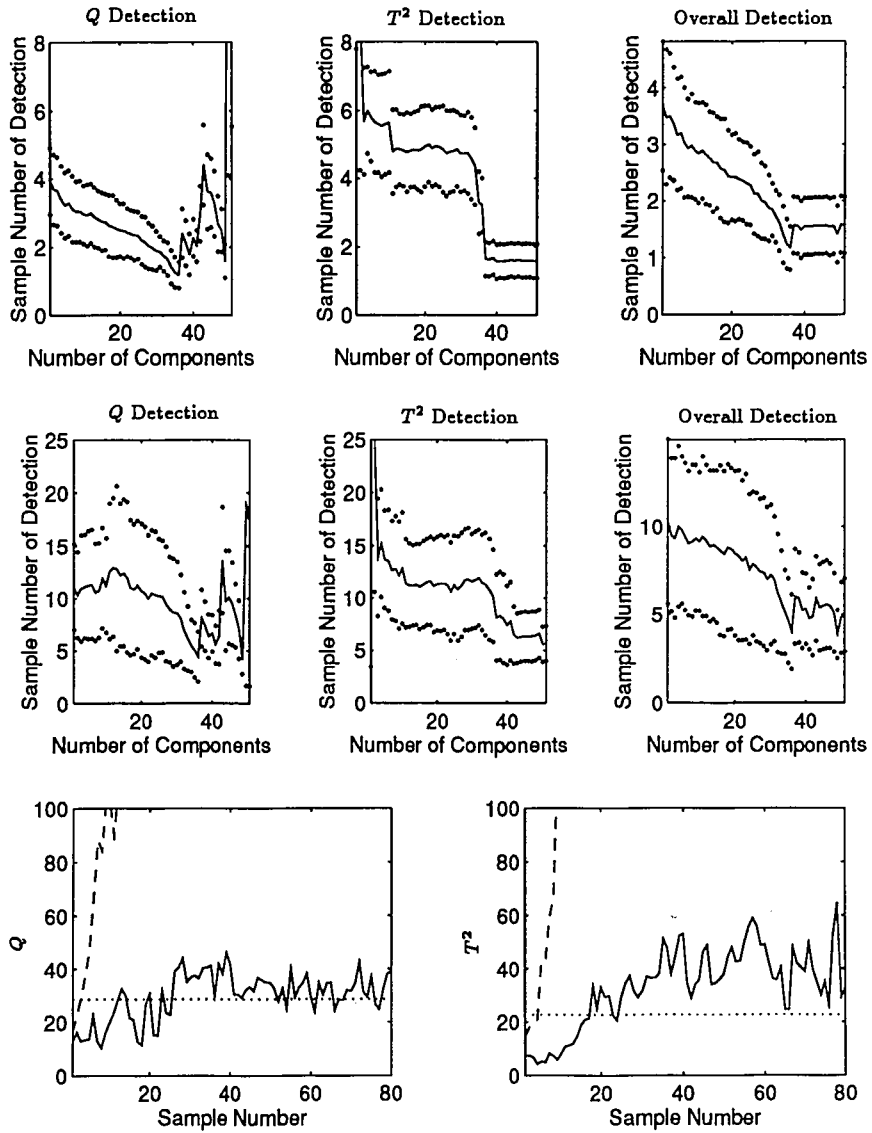


Figure B.1: Speed of Detection versus Number of Components in the PCA Model. Disturbance 1 (top plots), Reduced Magnitude Disturbance 1 (middle plots), Monitoring Plots (bottom).

APPENDIX B. SPEED OF DETECTION

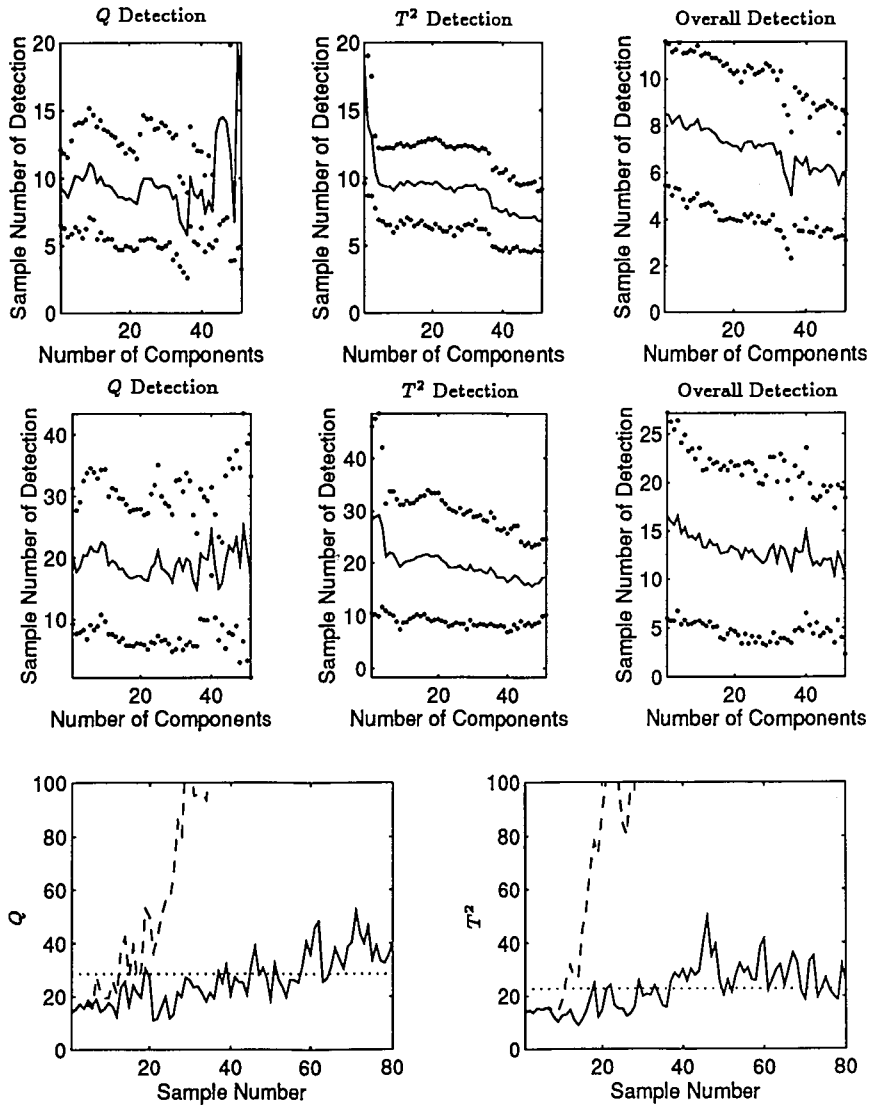


Figure B.2: Speed of Detection versus Number of Components in the PCA Model. Disturbance 2 (top plots), Reduced Magnitude Disturbance 2 (middle plots), Monitoring Plots (bottom).

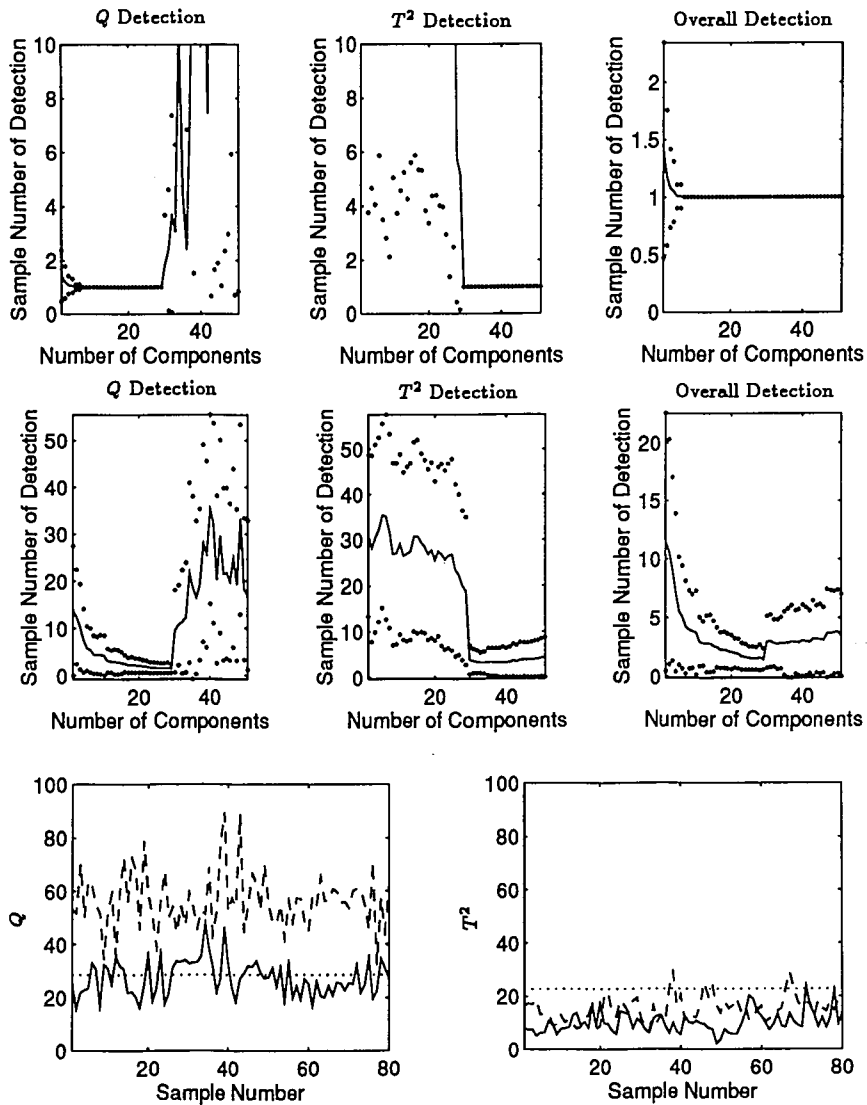


Figure B.3: Speed of Detection versus Number of Components in the PCA Model. Disturbance 4 (top plots), Reduced Magnitude Disturbance 4 (middle plots), Monitoring Plots (bottom).

APPENDIX B. SPEED OF DETECTION

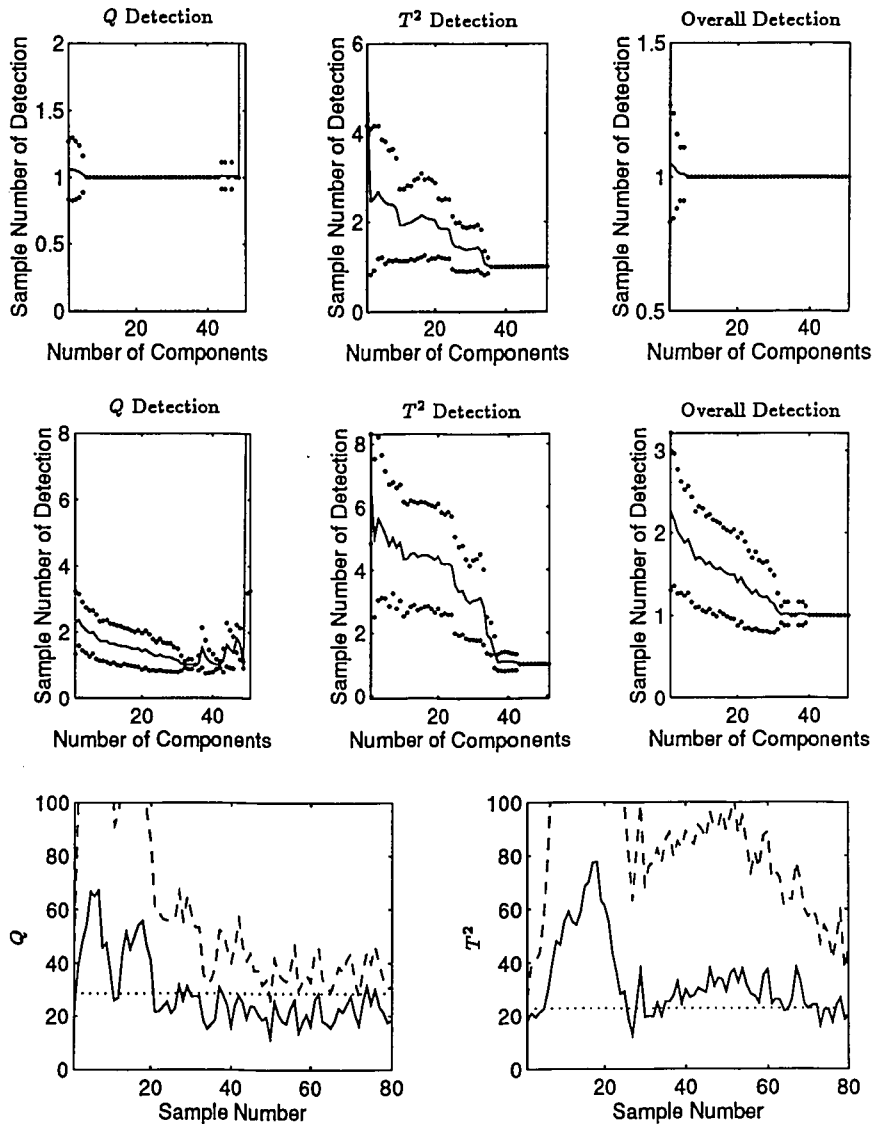


Figure B.4: Speed of Detection versus Number of Components in the PCA Model. Disturbance 5 (top plots), Reduced Magnitude Disturbance 5 (middle plots), Monitoring Plots (bottom).

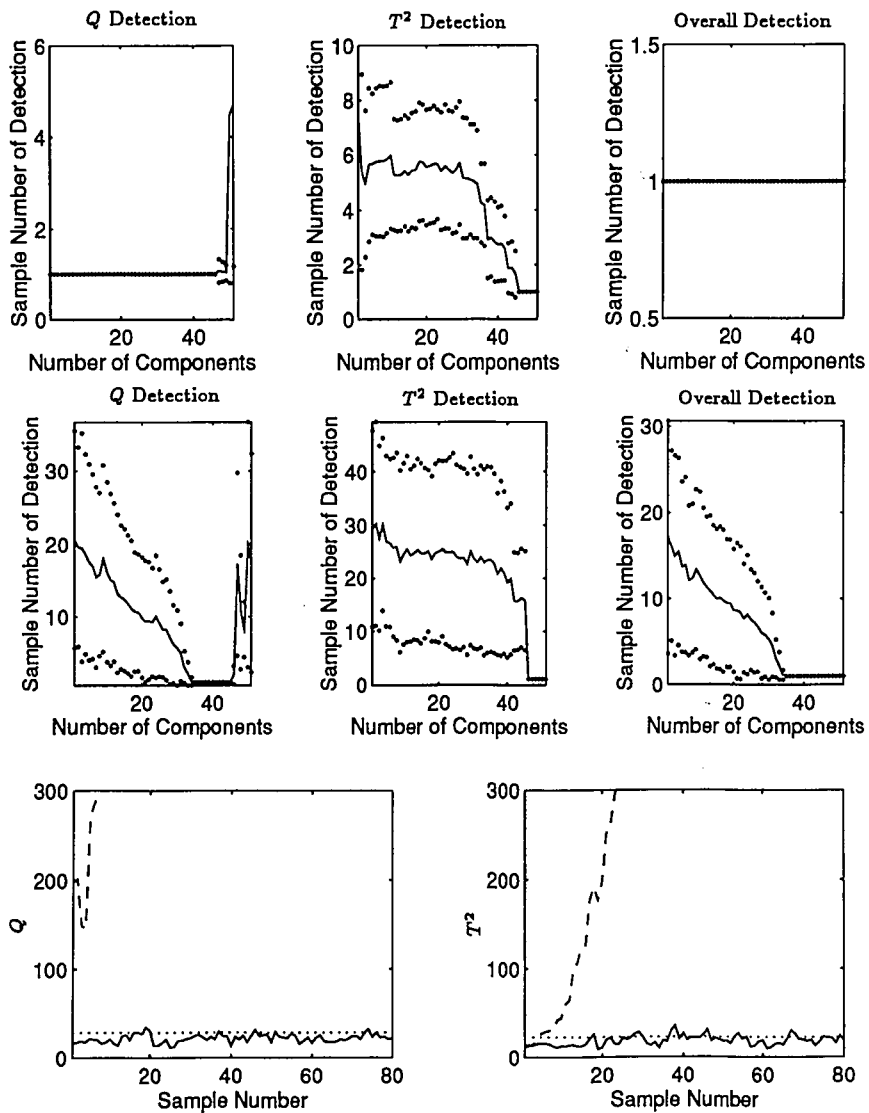


Figure B.5: Speed of Detection versus Number of Components in the PCA Model. Disturbance 6 (top plots), Reduced Magnitude Disturbance 6 (middle plots), Monitoring Plots (bottom).

APPENDIX B. SPEED OF DETECTION

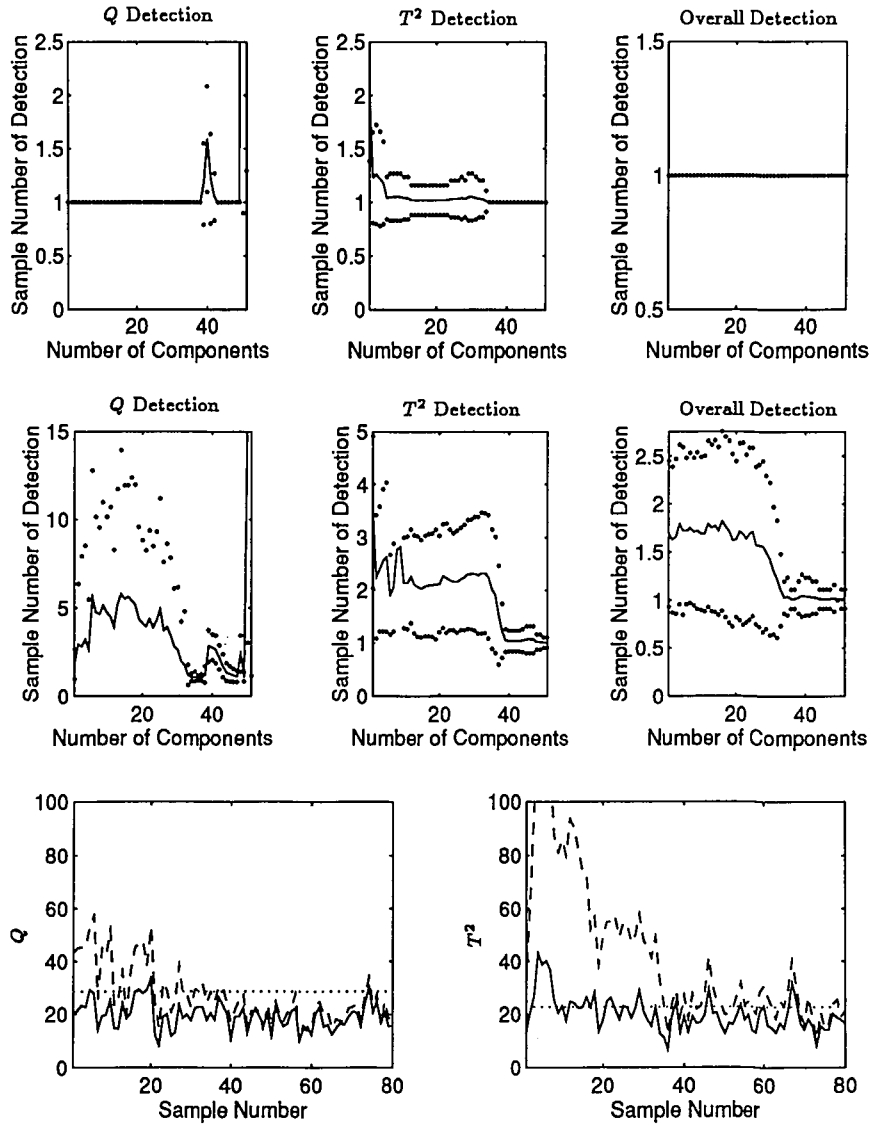


Figure B.6: Speed of Detection versus Number of Components in the PCA Model. Disturbance 7 (top plots), Reduced Magnitude Disturbance 7 (middle plots), Monitoring Plots (bottom).

Appendix C

Decentralized Charts

It was not possible to present all of the decentralized monitoring results in the main text due to the large number of examples and plots. In this appendix, the remaining disturbances are represented as further illustrations of the technique.

Each Figure is comprised of a series of plots. The top six plots represent Q charts for each of the decentralized units defined in Chapter 3. The bottom six plots represent T^2 charts. There are two figures for each disturbance investigated, one for full magnitude and one for reduced magnitude. Disturbances 1 and 6 are at 20% of the original magnitude, and disturbances 4, 5 and 7 are at 50% of the original. Disturbance 2 is activated at two locations in the encrypted simulation code, and at each location the effect is reduced to 20% of the original magnitude. Control limits based on 95 and 99% type I error risk are plotted as dashed lines in both charts. A circle indicates the sample which is the first to violate the control limits after the initiation of the disturbance. The time of this detection is provided beneath each chart.

APPENDIX C. DECENTRALIZED CHARTS

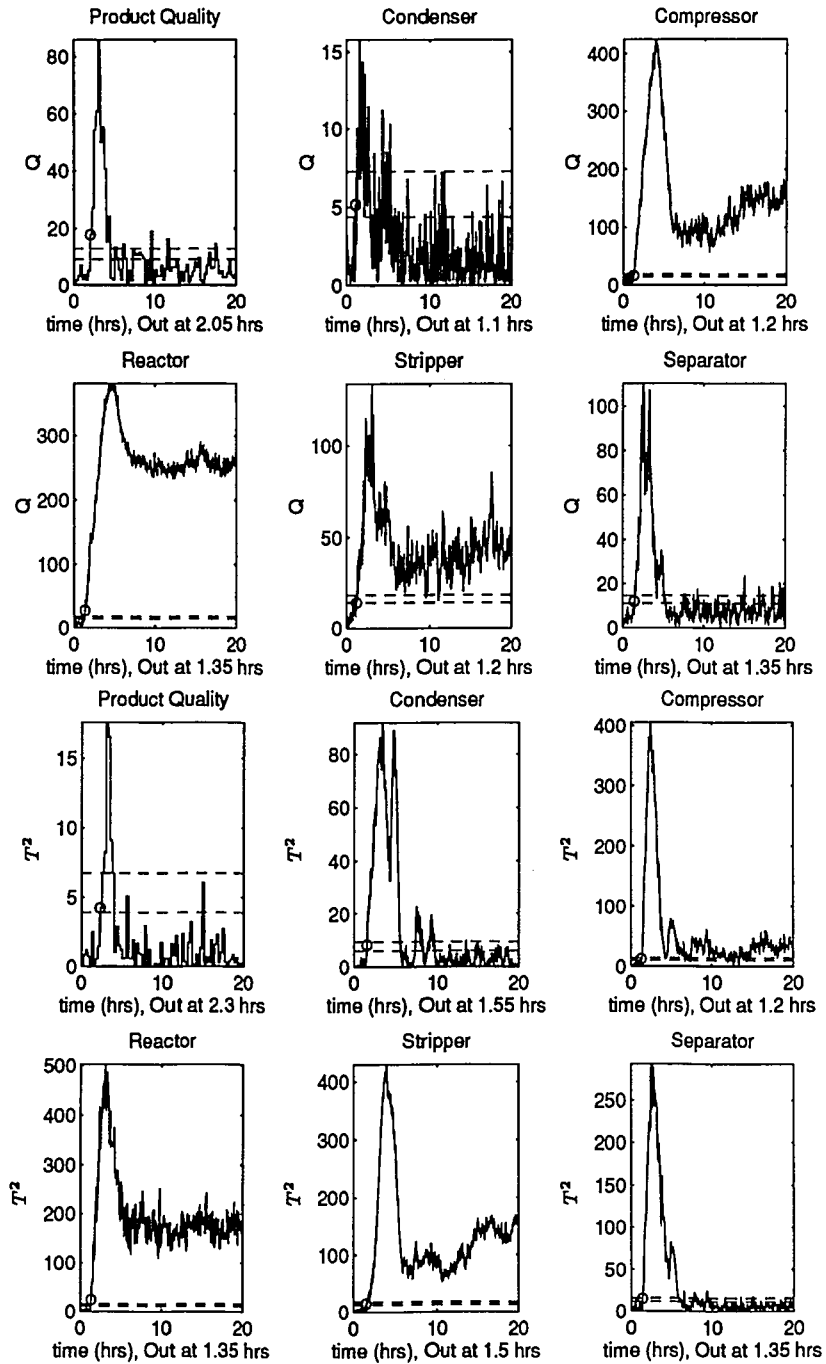


Figure C.1: Decentralized Monitoring of TE Disturbance #1

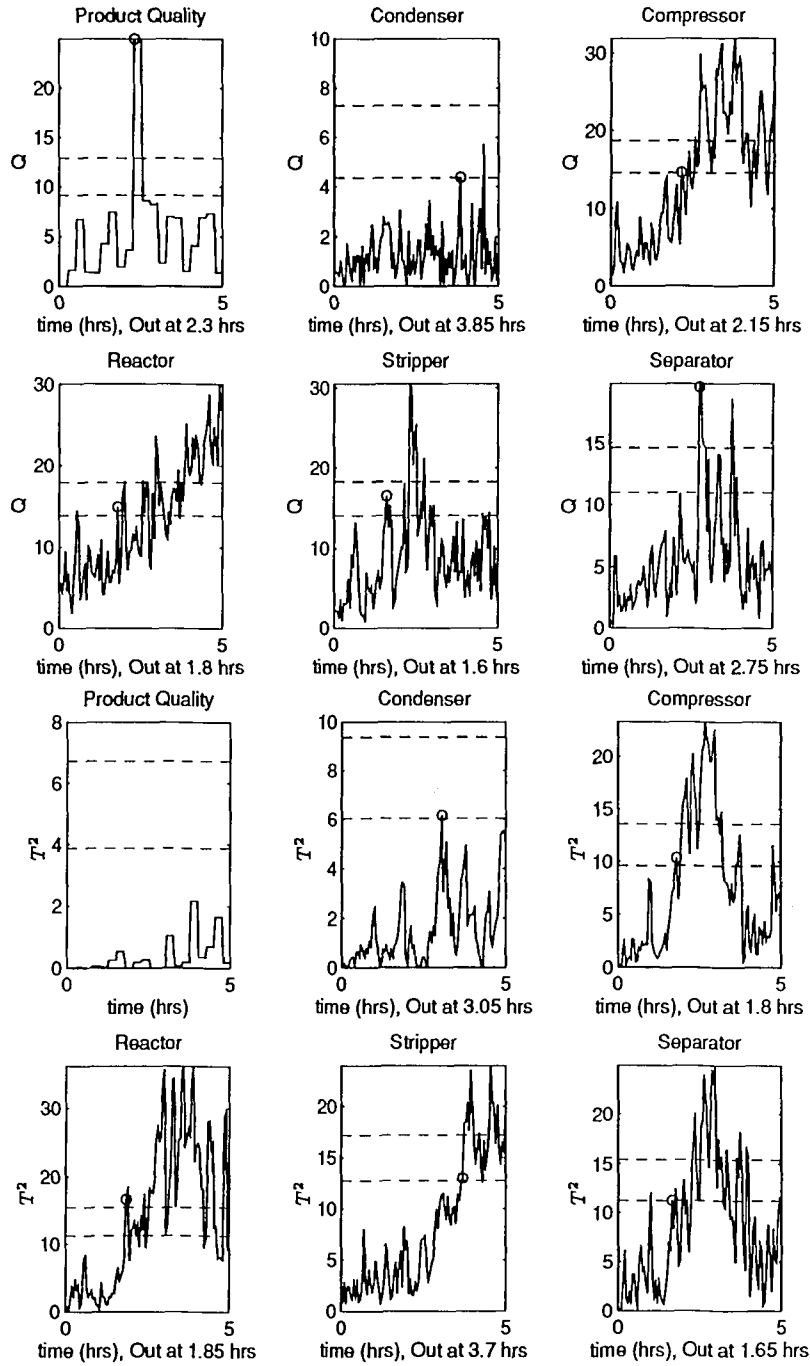


Figure C.2: Decentralized Monitoring of TE Reduced Magnitude Disturbance #1

APPENDIX C. DECENTRALIZED CHARTS

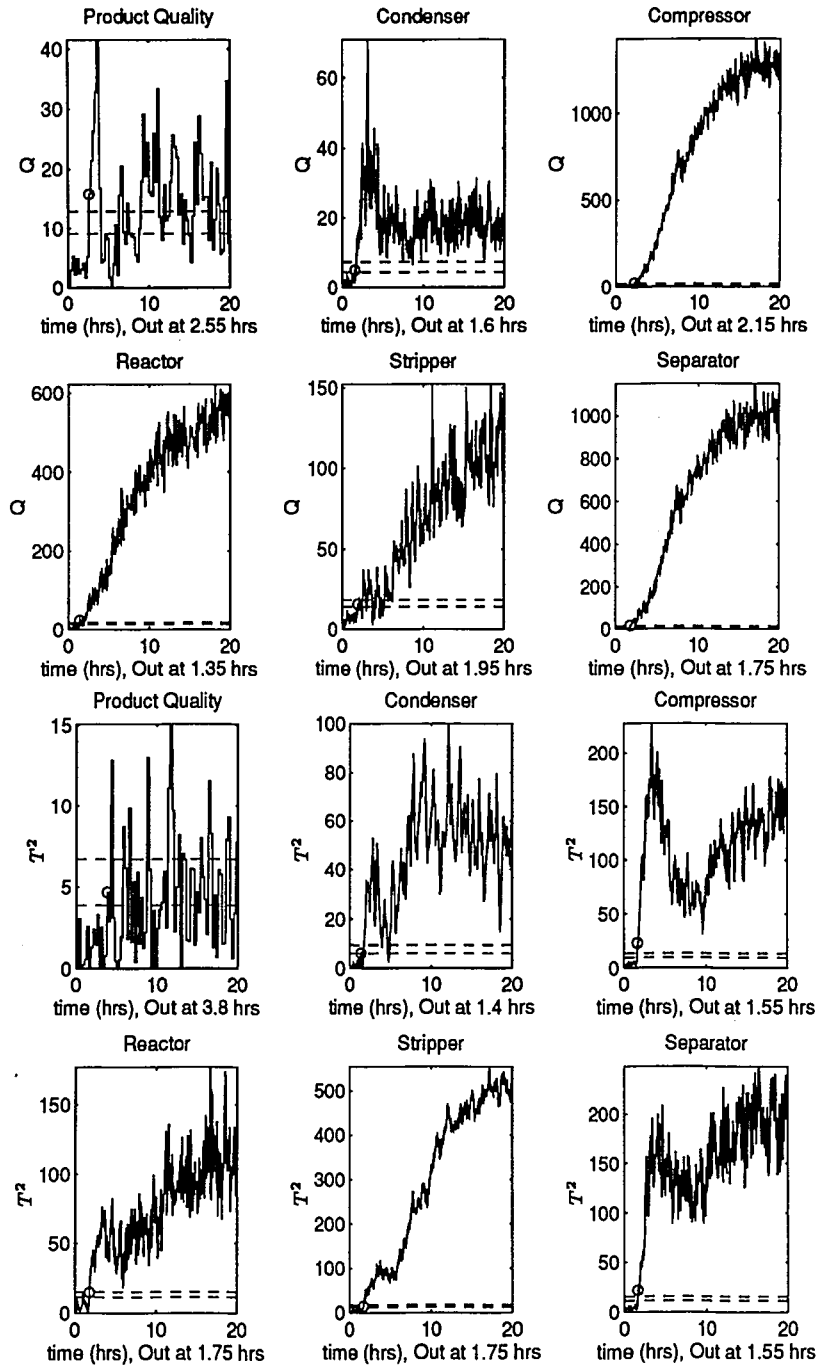


Figure C.3: Decentralized Monitoring of TE Disturbance #2

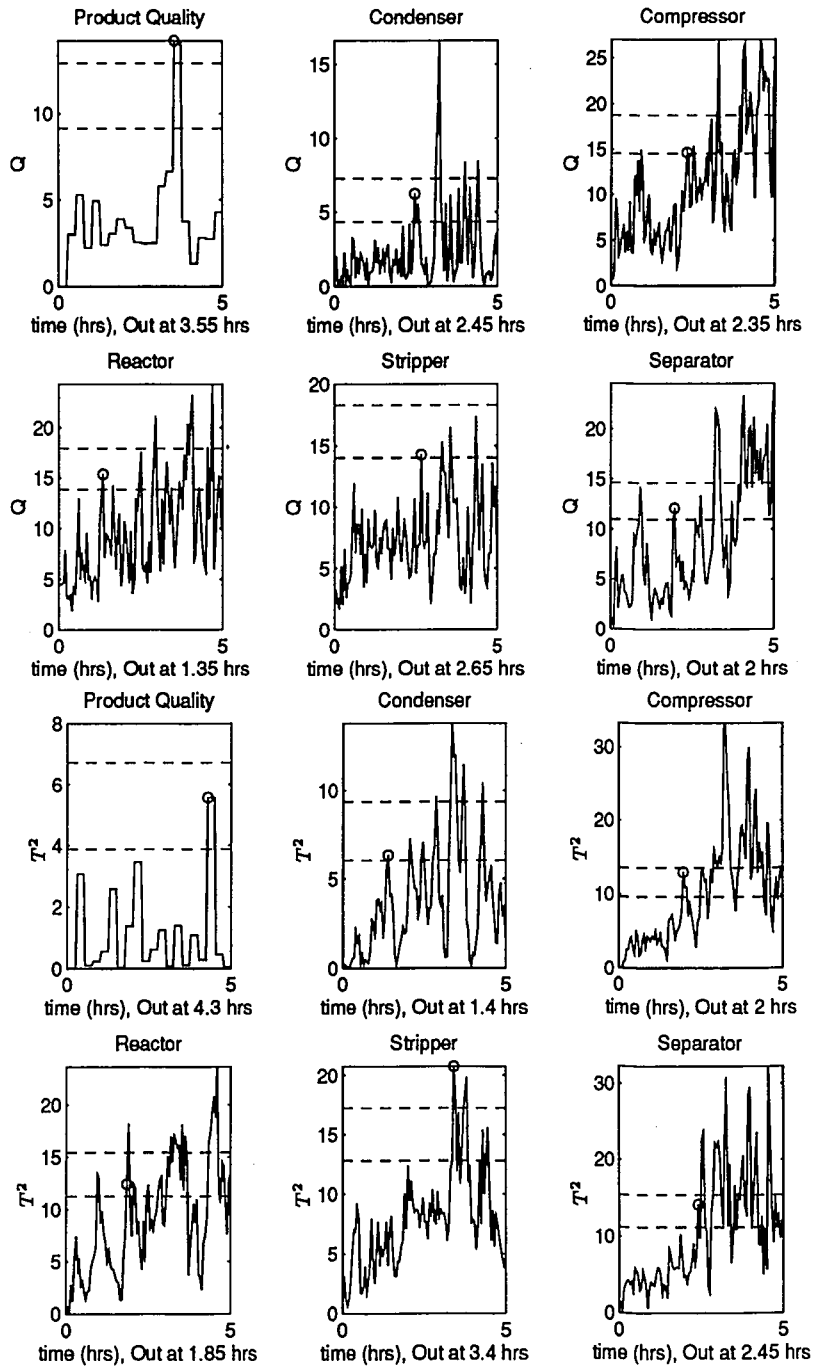


Figure C.4: Decentralized Monitoring of TE Reduced Magnitude Disturbance #2

APPENDIX C. DECENTRALIZED CHARTS

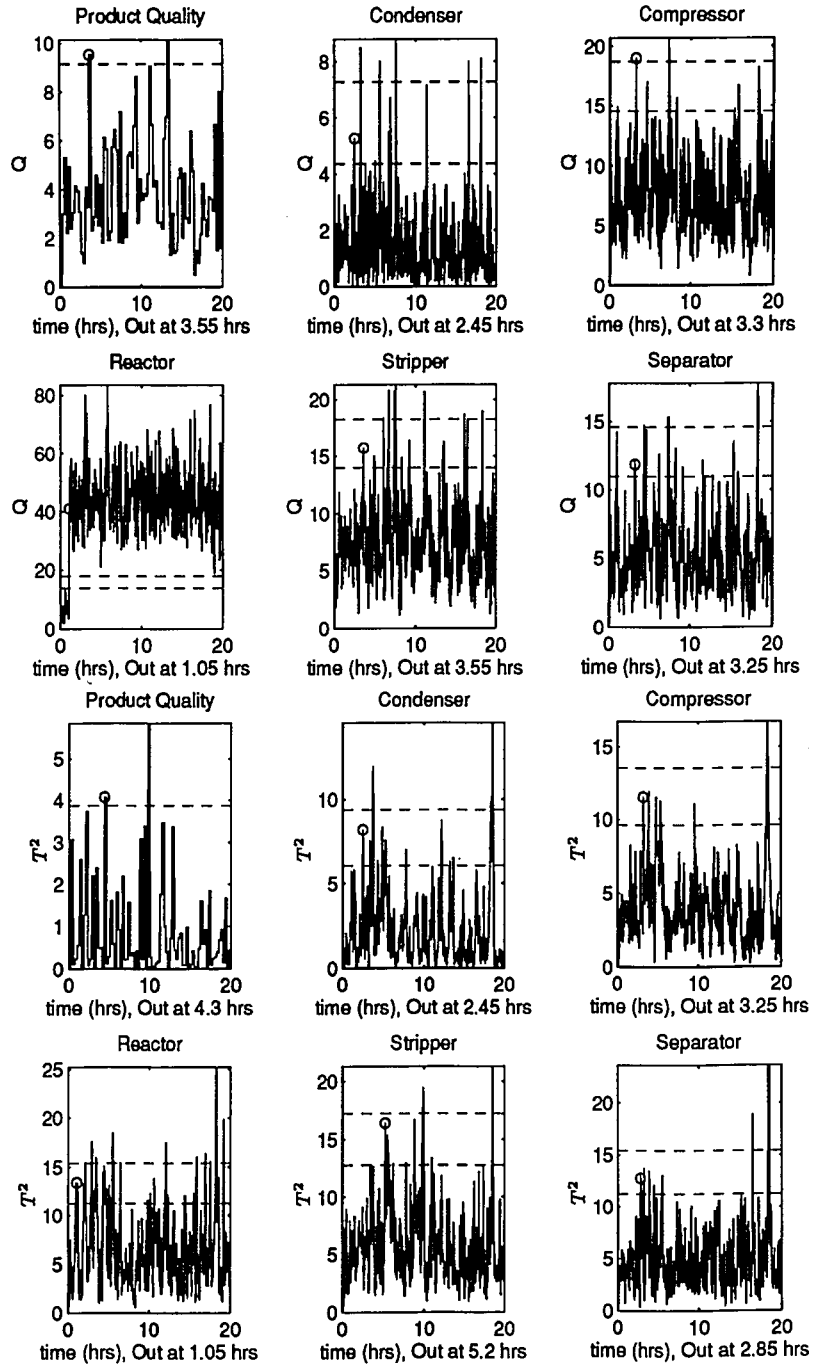


Figure C.5: Decentralized Monitoring of TE Disturbance #4

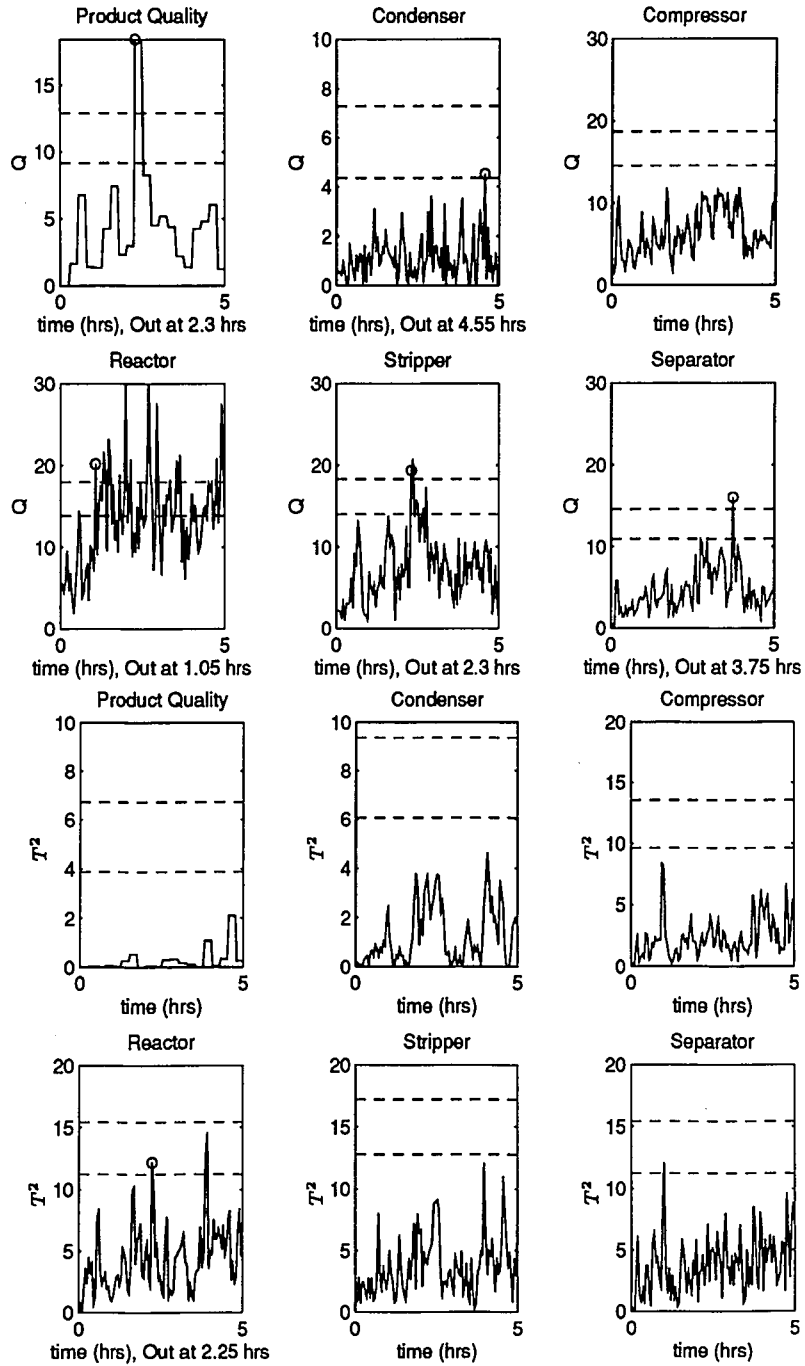


Figure C.6: Decentralized Monitoring of TE Reduced Magnitude Disturbance #4

APPENDIX C. DECENTRALIZED CHARTS

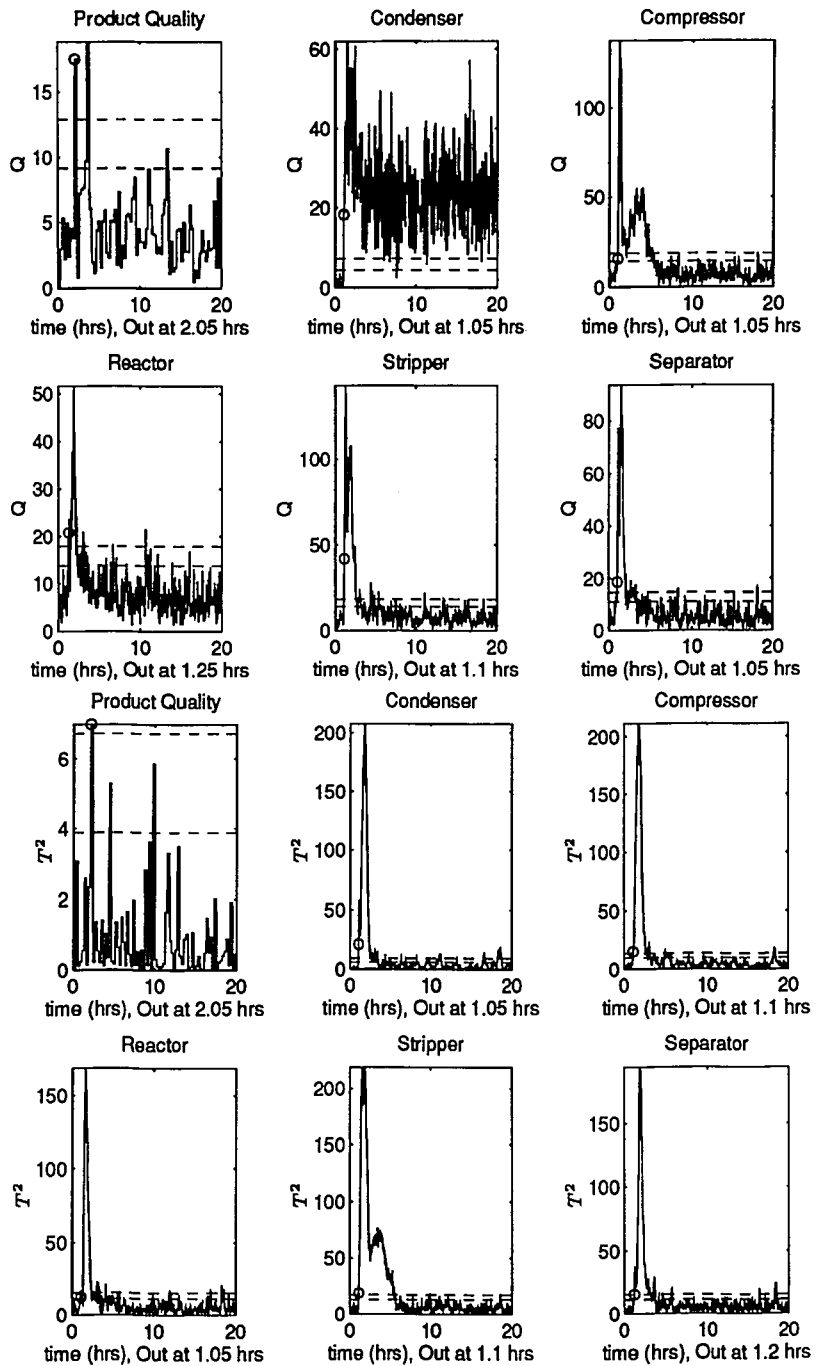


Figure C.7: Decentralized Monitoring of TE Disturbance #5

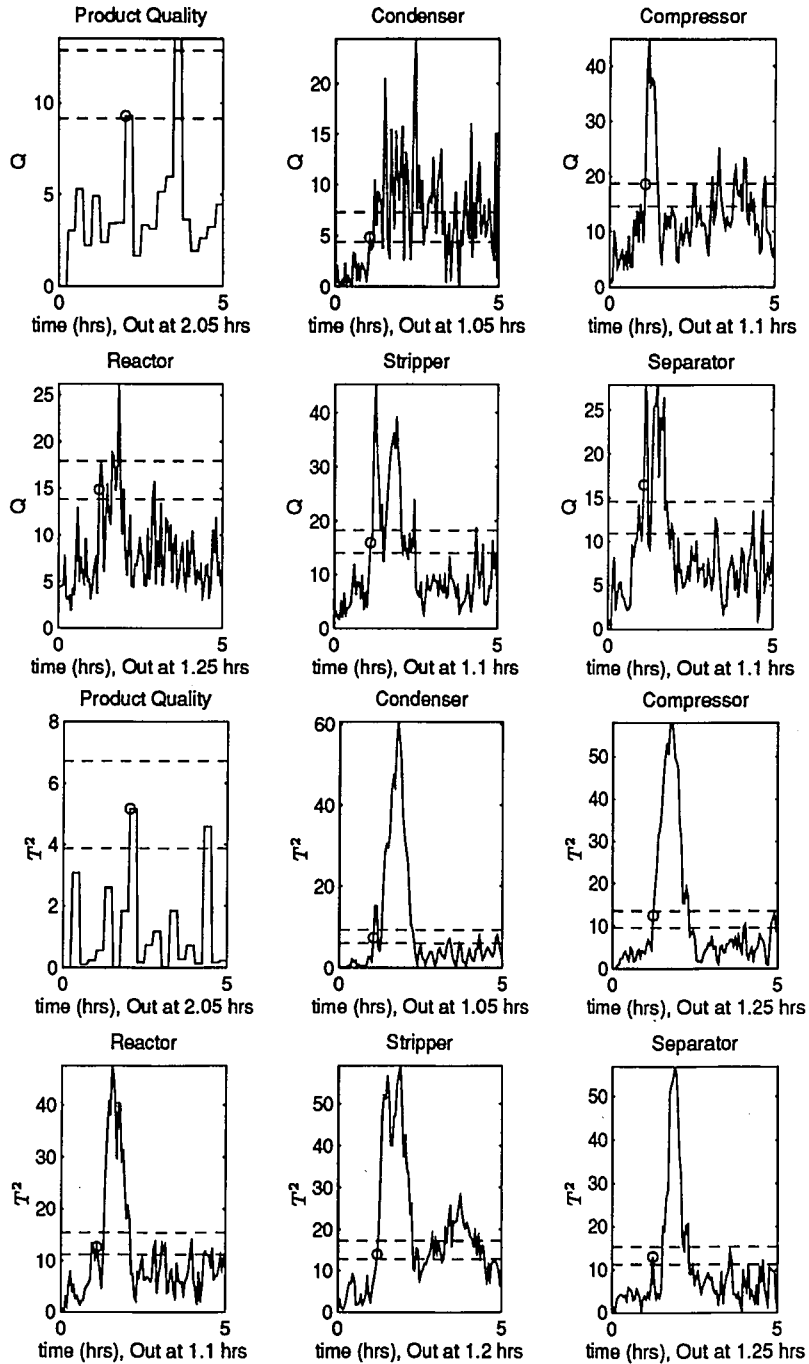


Figure C.8: Decentralized Monitoring of TE Reduced Magnitude Disturbance #5

APPENDIX C. DECENTRALIZED CHARTS

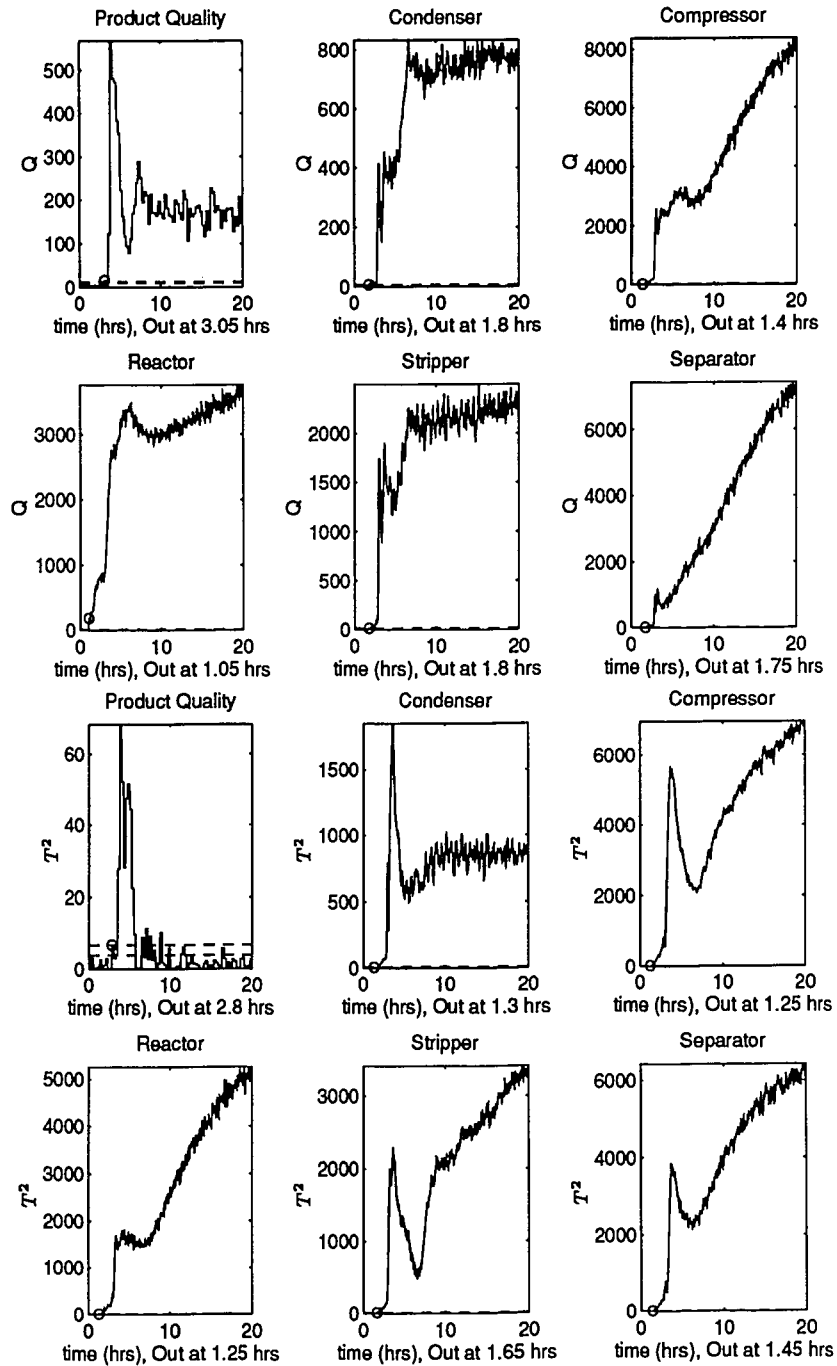


Figure C.9: Decentralized Monitoring of TE Disturbance #6

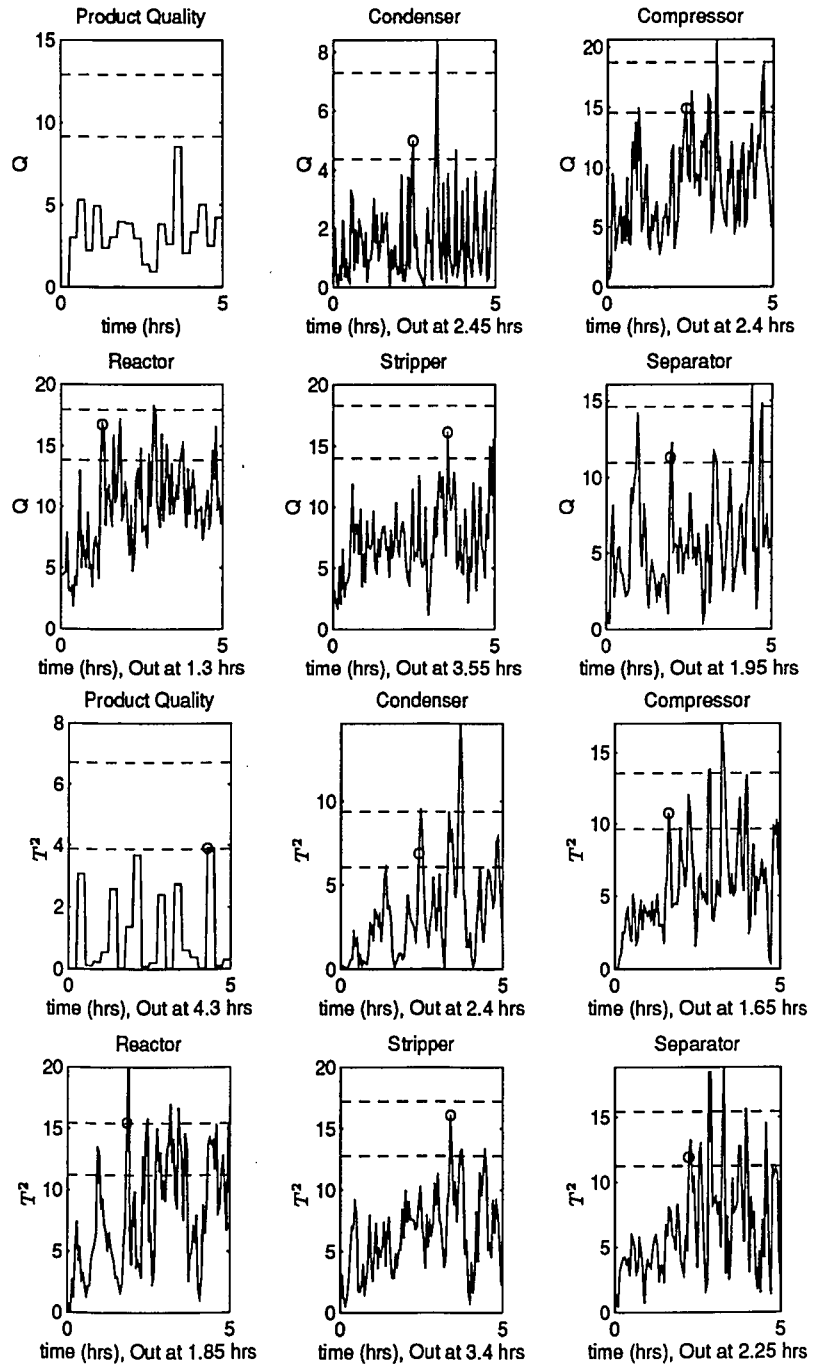


Figure C.10: Decentralized Monitoring of TE Reduced Magnitude Disturbance #6

APPENDIX C. DECENTRALIZED CHARTS

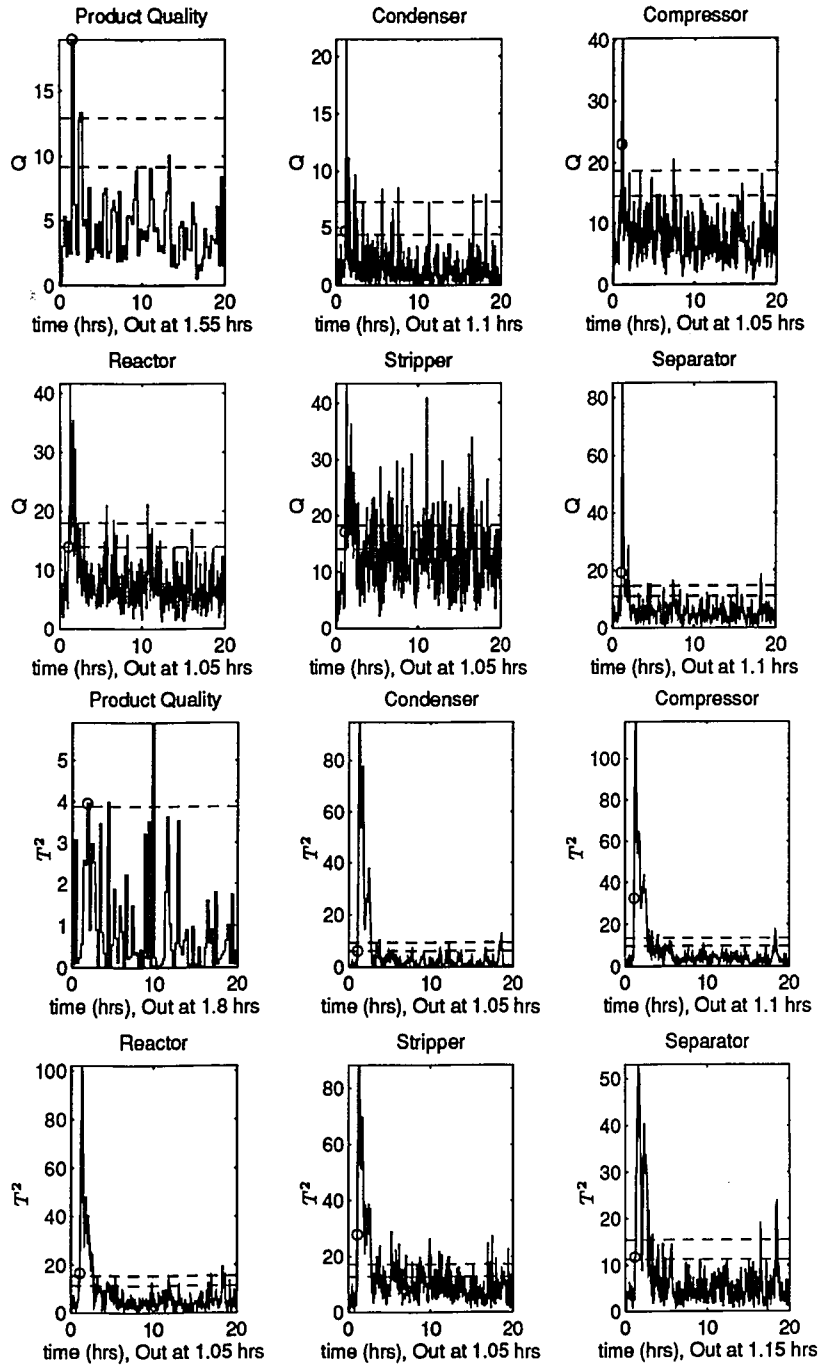


Figure C.11: Decentralized Monitoring of TE Disturbance #7

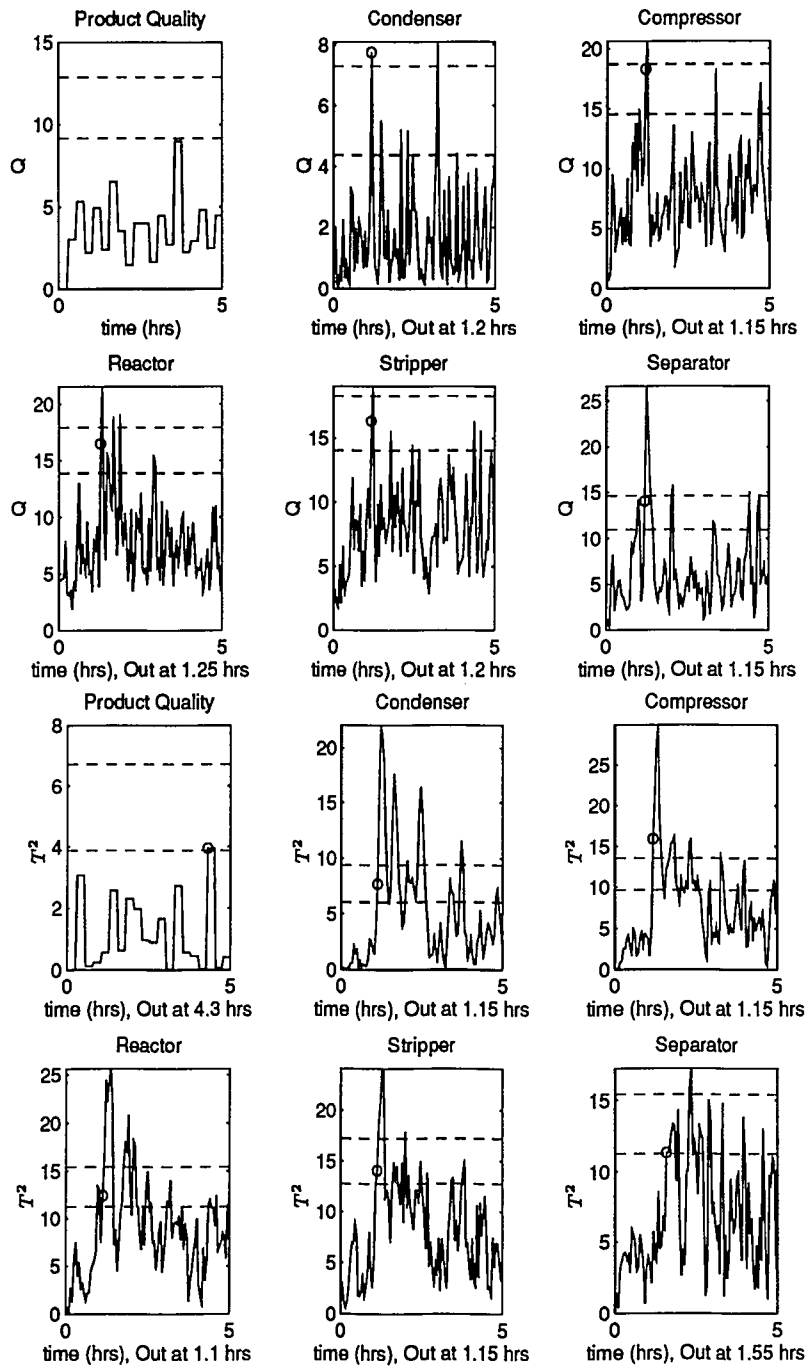


Figure C.12: Decentralized Monitoring of TE Reduced Magnitude Disturbance #7

APPENDIX C. DECENTRALIZED CHARTS

Vita

Name: David M. Himes
Date of Birth: January 18, 1969
Place of Birth: Ridgewood, New Jersey, USA
Parents: David L. Himes and Michelle M. Himes

Education: **B. S. Chemical Engineering, May 1992**
The Pennsylvania State University, University Park, PA
Cooperative Education Program
Air Products and Chemicals, Allentown, PA – May 91-Aug 91
Air Products and Chemicals, Allentown, PA – Aug 90-Dec 90
Air Products and Chemicals, Elkton, MD – Jan 90-May 90

M. S. Chemical Engineering, May 1995 anticipated
Lehigh University, Bethlehem, PA

Papers:

“Determination of the Number of Principal Components for Disturbance Detection and Isolation.” Personally presented at the 1994 American Control Conference.

“Decentralized PCA Models in Multivariate Statistical Process Control.” Presented at the November 1994 AIChE Annual Meeting.

**END
OF
TITLE**